

AD-A045 378

NAVAL ACADEMY ANNAPOLIS MD
PERFORMANCE ANALYSIS OF A MODIFIED INTERNAL COMBUSTION ENGINE.(U)

F/G 21/7

MAY 77 T L WHITED

UNCLASSIFIED

USNA-TSPR-90

NL

1 OF 1
AD
A045378L



AD A 045378

A TRIDENT SCHOLAR
PROJECT REPORT

NO. 90

"PERFORMANCE ANALYSIS OF A
MODIFIED INTERNAL COMBUSTION ENGINE"



UNITED STATES NAVAL ACADEMY
ANNAPOLIS, MARYLAND
1977

AD No. —
DDC FILE COPY

This document has been approved for public
release and sale; its distribution is unlimited.

DDC
RECEIVED
OCT 20 1977
D

U.S.N.A. - Trident Scholar project report; no. 90 (1977)

"Performance Analysis of a Modified
Internal Combustion Engine"

A Trident Scholar Project Report

by

Midshipman Tim L. Whited, Class of 1977

U. S. Naval Academy

Annapolis, Maryland

ACCESSION for	
NTIS	White Section <input checked="" type="checkbox"/>
DDC	Buff Section <input type="checkbox"/>
UNANNOUNCED	<input type="checkbox"/>
JUSTIFICATION.....	
BY.....	
DISTRIBUTION/AVAILABILITY CODES	
Dist.	AVAIL. and/or SPECIAL
A	

A. A. Pouring
A. A. Pouring
Professor
Aerospace Engineering Department

Accepted for Trident Scholar Committee

Chairman
Chairman

23 MAY 77

Date

DISTRIBUTION STATEMENT A

Approved for public release;
Distribution Unlimited

DDC
RECEIVED
OCT 20 1977
RECEIVED
D

TABLE OF CONTENTS

I.	ABSTRACT.....	1
II.	INTRODUCTION.....	2
III.	COMBUSTION WITH PRESSURE EXCHANGE	
	1. Experimental Pressure Behavior, Previous Work..	13
	2. Experimental Observations, Transparent Engine..	17
	3. Experimental Observations, Square Transparent Engine.....	18
IV.	FUTURE WORK.....	31
	REFERENCES.....	32
	APPENDIX I.....	33
	APPENDIX II.....	51
	APPENDIX III.....	75

I. ABSTRACT

The purpose of this study is to provide optical and other information on the processes undergone in the combustion and balancing chambers of the Naval Academy Heat Balanced Engine (NAHBE). In the NAHBE engine a pressure exchange cap is fitted on top of the piston to form a balancing chamber underneath. The pressure exchange between expansion and compression waves generated by this apparatus permits lower combustion temperatures and pressures, along with a significant decrease in pollutants emitted by the engine.

The combustion cycle resulting from the pressure exchange cap is a combination of both the OTTO and Diesel cycles, with added advantages not found in either of these two cycles. Previous laboratory results have indicated: (1) up to 25% reduction of fuel consumption, (2) reduction in peak operating pressures from 660 to 470 psi and exhaust temperature reduction on the order of 50°F, (3) over 90% reduction in pollutants (carbon monoxide, hydrocarbons, and nitrogen oxides), depending on load and compression ratio, (4) multifuel capability (low octane gasoline, fuel oil, alcohol and water, alcohol and charcoal), and (5) significant noise reduction.

In this preliminary investigation high-speed photography was utilized for visualization of the processes,

under consideration. To facilitate the use of optical methods for this and future investigations an existing transparent engine, the Megatech Mark III, was redesigned by Dr. Bruce H. Rankin. The cylindrical piston and cylinder were replaced by a square piston and cylinder. This modification allows optical methods to be used by minimizing the refraction and reflection of light passing through the cylinder.

It is the specific purpose of this study to verify that pressure exchange is taking place and to provide information that will lead to the optimization of the NAHBE cycle.

II. INTRODUCTION

Preliminary research developments (1) have already achieved several significant goals. It has been demonstrated that the NAHBE cycle has a natural process of combustion characteristic of the OTTO cycle with high compression ratio, rich mixtures and the efficiency and total fuel oxidation of the Diesel. However, the cycle does not have the high pressures and temperatures and the knock tendency of the OTTO, nor the high mechanical compression and smoke limitations of the Diesel. The preliminary experimental investigations have already demonstrated that the new controlled heat balanced cycles can avoid exhaust-

ing pollutants to the environment by utilizing a clean, time dependent process of combustion with pressure exchange. Thus, it is the overall objective of this study to show that pressure exchange is indeed the process responsible for the time dependent combustion that occurs in the NAHBE engine (5).

The research conducted by the author represents just a part of the team effort being exerted on the NAHBE engine. The research team also includes Dr. A. A. Pouring, Richard F. Blaser, Dr. B. H. Rankin, and Dr. E. L. Keating. Just as information gained through this experiment will be used in other research work to optimize the NAHBE cycle, reference will be made to results already obtained by other members of the research team. Appendix II contains quantitative data obtained using a single-cylinder CFR engine modified to the NAHBE configuration.

This report gives the state of the art of the Naval Academy Heat Balanced Engine in terms of its theoretical basis, laboratory tests of a Combustion Fuel Research (CFR) engine, preliminary demonstration of a multi-cylinder engine, and optical testing of a single-cylinder, transparent engine.

The many resources of the Division of Engineering and Weapons of the United States Naval Academy, the new theoretical understanding of the process proposed by Dr. Pouring,

the invaluable experience and help of the Technical Support Division as well as the Computer Aided Design and Graphics Group have all contributed to further the understanding of the heat balanced engine concept. Its early theoretical basis and proposed practical application were first presented in June 1974 (1).

The pressure exchange interaction between the cyclinder chambers as proposed by Dr. Pouring (3) has supplied governing parameters for this non-equilibrium process of combustion. Laboratory comparison of the performance of a standard and a modified single-cylinder transparent engine (Megatech Mark III, Figures 1,2) has given visual evidence that this non-steady process cannot be analyzed within the domains of equilibrium thermodynamics and the classic energy equations for chemical reactions of the combustion processes.

In addition to the transparent engine modification a 1938 (AD) L-Head four-cylinder Continental engine was modified and operated in a dynamometer. Only two days labor were required for this modification, being performed by technicians who are in no way automotive specialists. The simplicity of the modification supports the expectation that future applications of this novel process will allow production within existing manufacturing processes.

To familarize the reader with the heat balanced engine

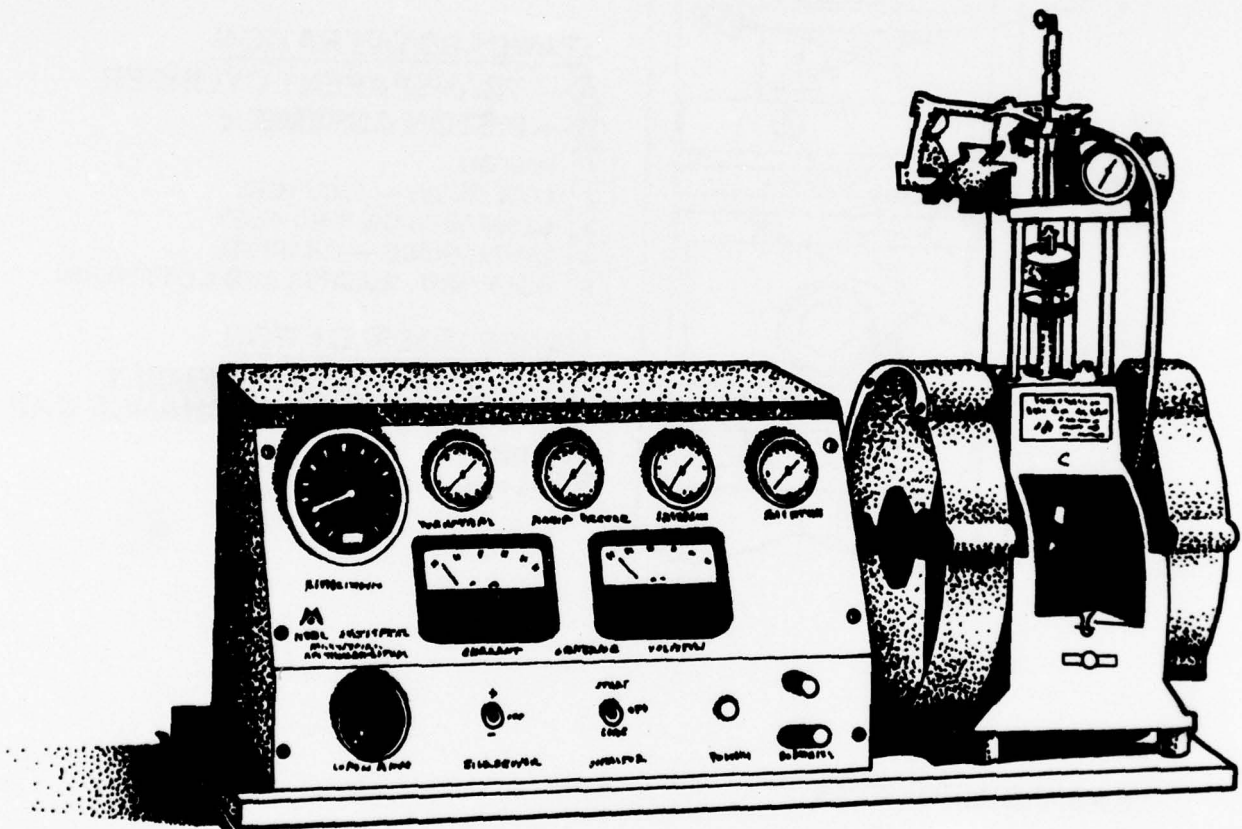
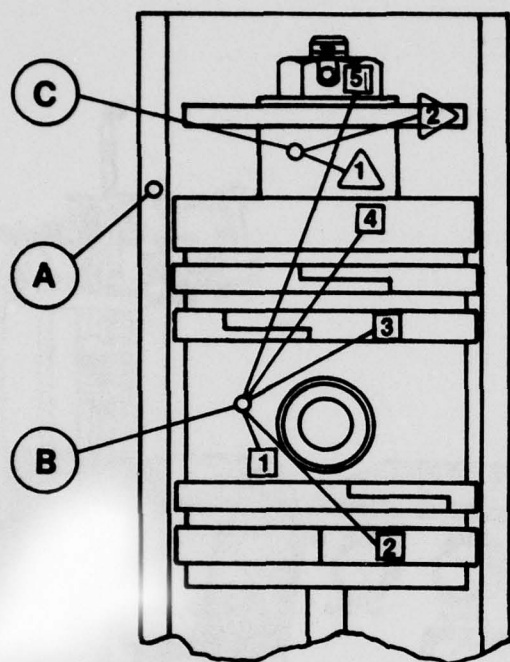


Fig. 1
THE MEGATECH MARK III



MEGATECH MARK III

STANDARD OPERATION

- (A) — TRANSPARENT CYLINDER
 (B) — PISTON ASSEMBLY

- | | |
|---|----------------------------------|
| 1 | PISTON |
| 2 | LOW GUIDE — GRAPHITE |
| 3 | COMPRESSION RING ASSY |
| 4 | UPPER GUIDE — GRAPHITE |
| 5 | BOLT, NUT, WASHER AND COTTER PIN |

NAHBE MODIFICATION

- (C) — PISTON HEAD ASSEMBLY
 OR PRESSURE EXCHANGE CAP

- | | |
|---|-------|
| 1 | RING |
| 2 | PLATE |

BASIC DIMENSIONS

DIA. — 1.625 in., 4.127 cm

STROKE — 2.000 in., 5.08 cm

SURFACE — 2.074 in², 13.38 cm²

VOLUME — 4.148 in³, 16.97 cm³

Fig. 2

Details of NAHBE Modification to MEGATECH MARK III

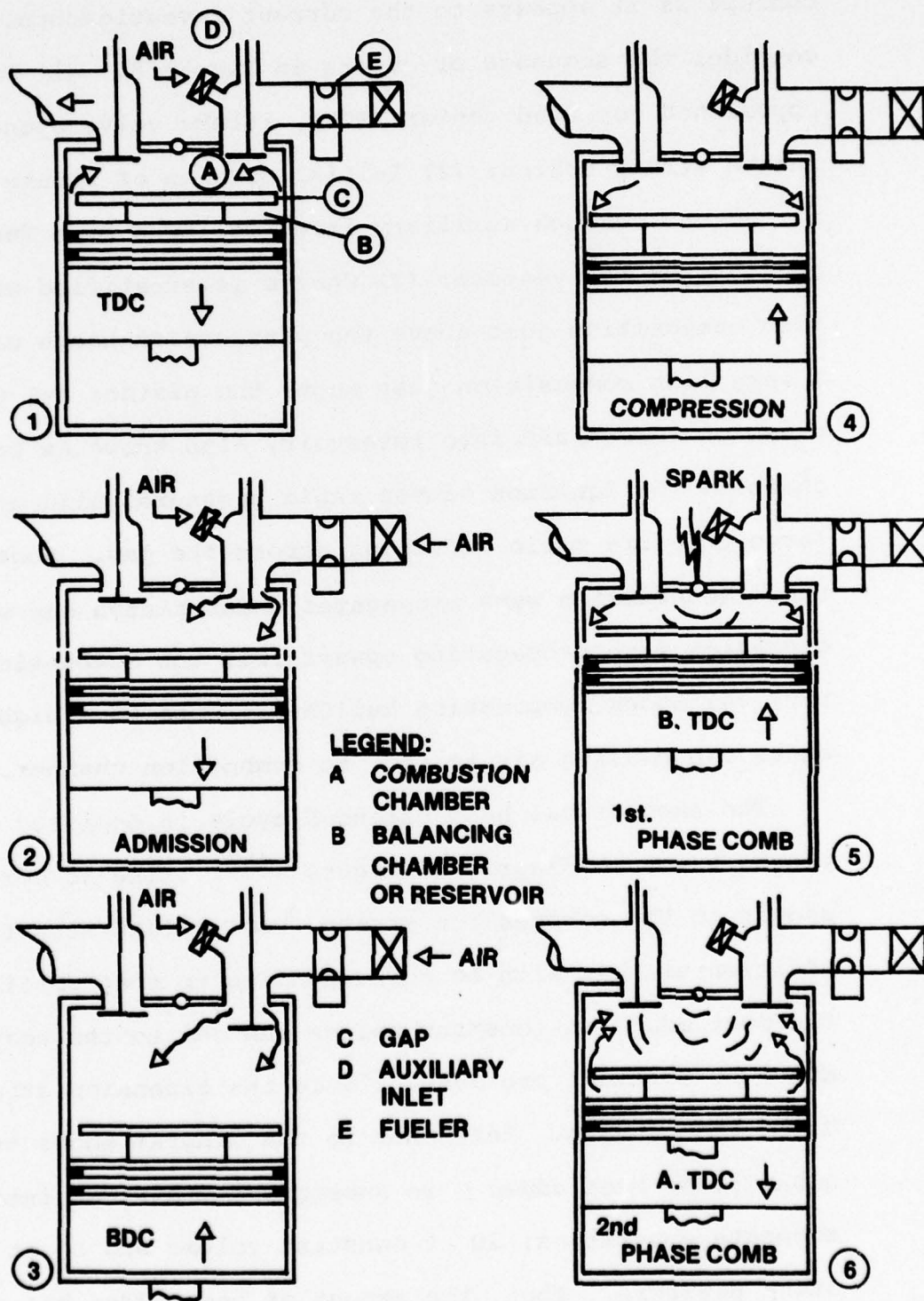


Fig. 3
Heat Balanced Engine Cycle

concept as it appears to the current investigators, consider the sequence of events in Figure 3. (1) Piston approached top dead center (TDC), intake valve opens and intake stroke begins; (2) Initial portion of intake stroke air enters through auxiliary inlet followed by a fuel-air charge from the venturi; (3) Charge is stratified with a rich composition just above the pressure exchange cap and a very lean composition just above the piston; (4) Compression forces air into reservoir, also known as balancing chamber; (5) Ignition causes rapid pressure build up with a large pressure ratio occurring across the gap. Subsequent shock compression wave propagates under piston cap with expansion wave propagating upward into the combustion chamber; (6) Shock compression builds pressure to a higher valve above cap causing air to flow to combustion chamber.

The theoretical heat balanced cycle is depicted by the pressure-volume diagram of Figure 4⁽⁵⁾. Line ab corresponds to the compression stroke, bcc' illustrates the addition of heat with bc corresponding to that portion of the heat added at constant volume and cc' to the heat added at constant pressure, c'd is the expansion stroke and da is the exhaust. Reference to the diagram shows the quantity of heat added Q is subsequently divided into two separate quantities, AQ at constant volume and BQ at constant pressure. Thus, the amount of heat added has not been

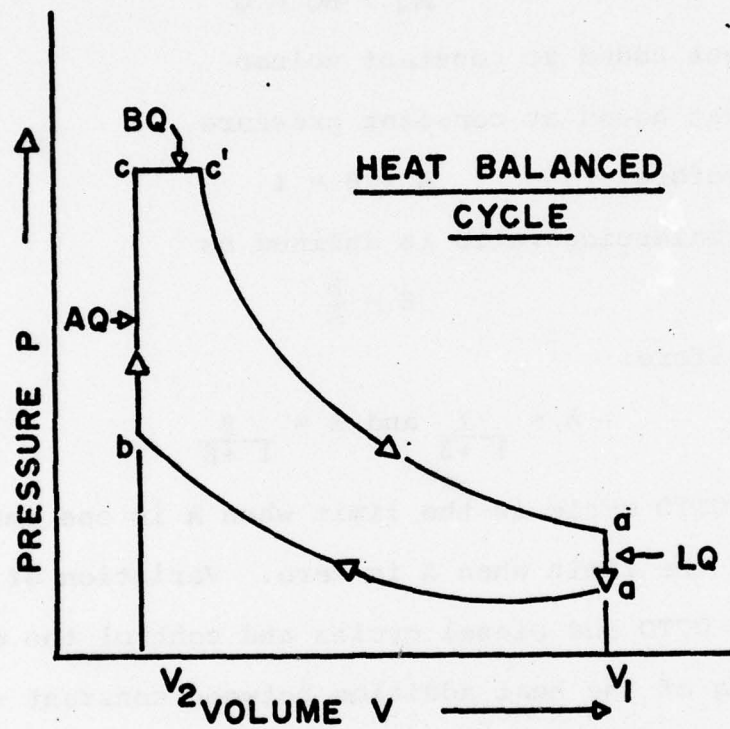


Fig. 4

Heat Balanced Cycle

changed; rather this parameter has merely been divided into two events. The following simplified equations set forth the relationship of the operating parameters of the heat balanced cycle

$$AQ + BQ = Q \quad (1)$$

AQ is heat added at constant volume

BQ is heat added at constant pressure

Therefore: $A + B = 1$

The balancing ratio is defined as

$$\beta = \frac{B}{A} \quad (2)$$

Therefore:

$$A = \frac{1}{1 + \beta} \text{ and } B = \frac{\beta}{1 + \beta}$$

The OTTO cycle is the limit when A is one and the Diesel cycle is the limit when A is zero. Variation of β will combine the OTTO and Diesel cycles and control the degree of balancing of the heat addition between constant volume and constant pressure. The efficiency of the heat balanced cycle is expressed as follows:

$$\begin{aligned} \eta_{\beta} &= \frac{Q - LQ}{Q} = \frac{AQ + BW - L AQ - L BQ}{Q} \\ \eta_{\beta} &= \frac{A AQ - L QA}{AQ} + B \frac{BQ - L QB}{BQ} \quad (3) \end{aligned}$$

Referring to the cycle efficiencies,

$$\eta_{\beta} = A \eta_v + B \eta_p ;$$

$$\eta_p = 1 - \left(\frac{1}{r_B}\right)^{k-1} \frac{\alpha_{Bk} - 1}{k(\alpha_B - 1)} \quad (4)$$

Calling $\gamma = \frac{P_3}{P_4}^{\frac{1}{k}}$, $r_B = \gamma r$ and $\alpha = V_C/V_C$, Figure 4.

The efficiency of the controlled heat balanced cycle is:

$$\eta_\beta = 1 - \left(\frac{1}{r}\right)^{k-1} \frac{1}{1+\beta} \left[1 + \beta \left(\frac{1}{\gamma}\right)^{k-1} \frac{\alpha_\beta^k - 1}{k(\alpha_\beta - 1)}\right] \quad (5)$$

The efficiency limits of the heat balanced cycle are those of the OTTO and diesel cycles with the same design compression ratio, or:

$$\eta_\beta \rightarrow 1 - \left(\frac{1}{r}\right)^{k-1}$$

when $\beta \rightarrow 0$ or $A \rightarrow 1$, OTTO cycle
 $B \rightarrow 0$

when $\beta \rightarrow \infty$ or $A \rightarrow 0$, Diesel cycle
 $B \rightarrow 1$

Thus, control of the pressure in the combustion process is achieved by the "balancing" chamber or air reservoir under the cap. The degree of balancing of combustion between "constant volume" and "constant pressure" process is controlled by varying the ratio of the volume below the cap to the volume above the cap at TDC, the balancing ratio. The balancing ratio is depicted in Figure 5 as V_B/V_A . The additional air pumped from the balancing chamber or air reservoir to the combustion chamber by shock compression prolongs the combustion process of pressure exchange.

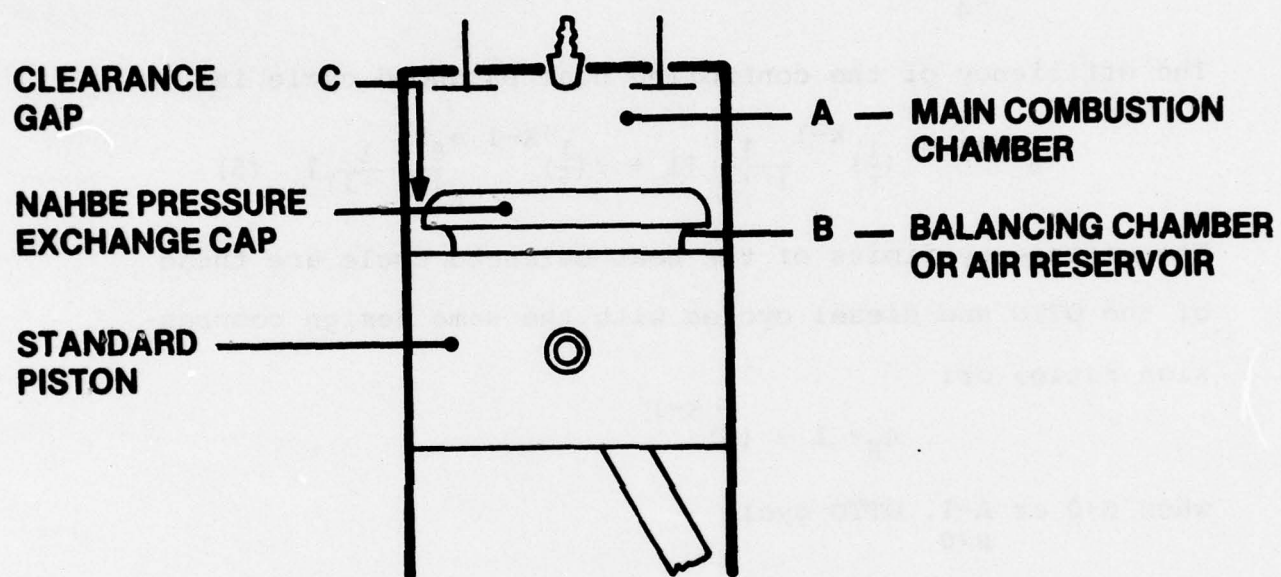


Fig. 5

Schematic of engine geometry

III. COMBUSTION WITH PRESSURE EXCHANGE

1. Experimental Pressure Behavior, Previous Work

The criteria for selecting a given geometry for demonstrating the feasibility of the Heat Balanced Cycle was originally determined from the basic concepts of equilibrium thermodynamics considering the flow of gases between two chambers, a primary and a secondary, was to provide a "relief" chamber for the primary combustion chamber. The geometries proposed initially, holes, valves and cavities (for example perforated piston caps) did not achieve the expected result. Material failure and heat transfer difficulties contributed to this lack of success. By broadening the experimental approach and assuming that the chamber could interact through the use of a narrow annular gap (rather than holes), a simple new geometry was adopted which gave the first indication of success (see Figure 5). After a few trial and error dimension changes involving the volumes above and below the pressure exchange cap and the gap between the cap and the cylinder wall the experimental data fully confirmed theoretical expectations and p-v diagrams much like those for a diesel were obtained.

For the analysis and evaluation of the characteristics of the cycle, piezoelectric transducers were used as pressure sensors. Two separate transducers were used for recording a p-v diagram and expanded view of the combustion

process with its related peak pressure. During the test, well-defined peaks or ripples appeared in the pressure recording. These covered the period of all the addition of heat from spark ignition to part of the expansion process (see Figure 6).

The appearance of the ripples in the pressure recordings at first were attributed to faulty instrumentation. However, when changes of transducers and their locations did not change the ripple pattern, it was accepted by the experimentors that the ripples were the combined result of the combustion process and the non-steady flow generated by the chamber geometry. In addition, the number of ripples observed further supports the pressure exchange concept. For a chamber length on the order of one inch, sound speed is on the order of 25,000 inches/sec and combustion lasts on the order of a millisecond.

$$n = \frac{25,000 \text{ inches/sec} \times 10^{-3} \text{ sec}}{1 \text{ inch}} = 25 \quad (6)$$

This number matches the approximate number of ripples observed per combustion stroke in oscilloscope traces.

This correlation between the number of ripples observed on the oscilloscope and the number calculated is indeed strong evidence that the ripples are the result of pressure exchange. Although the possibility existed that the ripples resulted from ground waves traveling through the cylinder walls and head, this explanation of the ripple

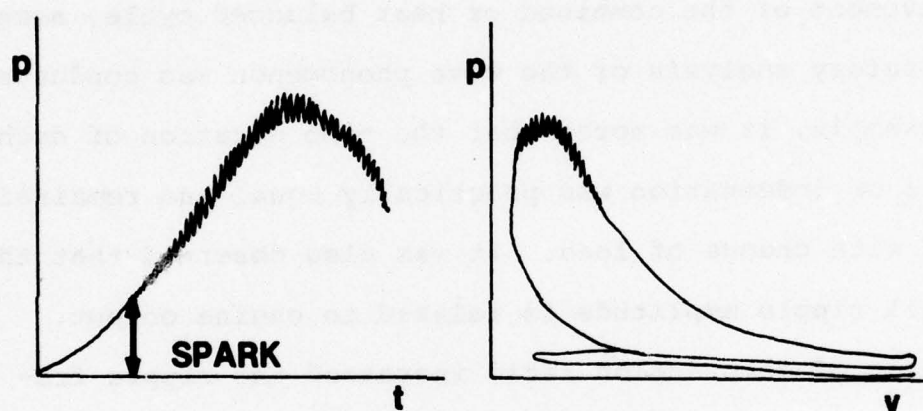


Fig. 6

Pressure Graphs

existence in pressure readings can be discounted because the number of ripples would change considerably. This is because the wave propagation speed through the cylinder would be much more than that through the gaseous environment within the cylinder.

Although the prevailing objective at the moment was achievement of the combined or heat balanced cycle, some exploratory analysis of the wave phenomenon was conducted. For example, it was noted that the time duration of each ripple or indentation was practically equal and remained equal with change of load. It was also observed that the overall ripple amplitude is related to engine output. Increase of compression ratio increased the ripple frequency and amplitude. Increase or decrease in gap size did not affect the frequency but inversely affected the amplitude. Lastly, it was found that a change of fuel did not change the frequency but it indicated that the amplitude is related to fuel flash characteristic. Alcohol gave a low amplitude while diesel fuel gave a higher amplitude ripple.

The mechanism proposed (3) to explain this new phenomenon is based on the concepts of non-steady gas dynamics (3,4) and is roughly analogous to the process observed in a shock tube. In a shock tube, rupture of a diaphragm supporting a high pressure gas from a low pressure gas

creates a shock wave which propagates through the tube compressing the low pressure medium. The shock wave is sustained by an expansion wave propagating into the high pressure medium. Pressure exchange (3) refers to the compression of one medium at the expense of the expansion of another.

It appears to the investigators that the ripples observed in their experiments could be attributed to pressure exchange. The ripples appeared when a solid cap is placed on the piston yet they were not present when a perforated disk was used. It was concluded that a compression wave, perhaps a shock wave, is driven under the piston cap when combustion causes the rapid pressure increase in the upper volume. Coincidentally, an expansion wave propagates into the combustion zone, dropping the pressure there. If the cap is perforated, immediate short circuiting of the pressure above and below the cap occurs and essentially no reduction of pressure nor ripple is observed.

2. Experimental Observations, Transparent Engine

The unusual characteristics of the heat addition process of the NAHBE have been demonstrated through the use of two single-cylinder transparent engines, one standard OTTO and the other modified to the NAHBE configuration (2).

Both engines have been operated under the same condi-

tions and direct visual comparison of the combustion phenomenon shows that they are totally different. The influence of the composition of the fuel-air mixture on the propagation of the flame in the media as a whole is very pronounced for the OTTO cycle. At best power, a white, very intense combustion propagates through the whole chamber at the composition. Orange is the basic color appearing in rich mixture and the characteristic blue color of total combustion is obtained only at very low loads with attendant lack of operational stability.

On the contrary, NAHBE combustion reflects excellent progression of molecular dissociation and the influence of pressure exchange at all engine loads. At maximum load a white central zone of fast molecular interaction is enclosed by a blue layer in which pressure exchange between chambers supplies oxygen for the ending the dissociation of fuel. When the engine output is reduced by reducing the supply of fuel, the white zone decreases in size but remains enclosed in a large blue zone. At very low load with little fuel, the white zone becomes a central point in an otherwise blue volume.

3. Experimental Observations, Square Transparent Engine

In this preliminary optical study, it is desired to investigate only qualitative aspects of the combustion

process of the NAHBE cycle. However, there will naturally be some reference made to quantitative observations in order to categorize some of the qualitative analysis that will be made.

As was expected, technical problems were encountered in operating the newly designed square version of the Megatech Mark III engine. (see Appendix I). Initially, a total running time of approximately five minutes was obtained, broken into $1-1\frac{1}{2}$ minute segments, before mechanical failure occurred. Mechanical friction resulted in the fracture of one of the pyrex glass cylinder walls. It was apparent that the failure was not related to thermal stress of the glass but the source of the mechanical interference could not be yet determined. After reassembly, the total running time again was about five minutes before failure again occurred. At this point, it was apparent that the piston was the source of the interference. At the same time the glass fractured, the graphite piston guide (upper) also developed a fracture. This fracture was the result of the difference in the coefficients of thermal expansion between the aluminum used in making the piston and the graphite out of which the piston guide was fabricated. Original design allowed no spacing between the piston guide and the piston. Consequently, as thermal expansion occurred and the piston expanded faster than the

guide, the piston guide fractured and produced a concentrated force on the glass. Subsequent glass failure resulted. The piston guide was altered to allow for the difference in thermal expansion between graphite and aluminum. A tolerance of 0.005" on each of the four inner sides of the piston guide was machined to permit the piston ample room to expand. Further engine operation has demonstrated that this source of mechanical interference has been eliminated in that no cracks have occurred in the piston guide exerting a concentrated force on the cylinder glass.

Although the source of mechanical interference was now removed, a different type of glass failure replaced the first type. Engine operating times before failure increased, but not by any large amount. To this date, two failures of the second type have occurred. The failure was a vertical crack in the glass, beginning at the top (nearest the cylinder head) and located in the middle of the glass wall in the horizontal dimension. Investigation of the failure indicated that the glass was failing in tension due to an oversight in design. As can be seen in the engine drawings, the glass cylinder walls are rigidly supported by the aluminum walls in the vertical direction. However, in the horizontal direction, only the bottom of the glass walls is supported. The top of the glass is only "supported" by the friction between the glass and the head

gasket. Consequently, when the pressure inside the cylinder exerted a force on the glass in an outward direction, the top part of the glass wall was essentially a beam supported at both ends with an evenly distributed force being applied. In this case, maximum deflection occurred at the middle (horizontally speaking) and was enough to produce a failure. Design modifications to correct this will provide rigid support to the glass at the upper edge and prevent this failure.

Due to early technical problems associated with the square version of the Megatech Mark III engine (see Appendix I) it became apparent that a lengthy run of the engine under constant conditions would be nearly impossible to obtain. As such, film footage of the high speed photography of the combustion process is comprised of several different operating conditions. However, it became apparent from the film that the single most important parameter in operating the engine in the NAHBE cycle was the fuel-to-air ratio of the fuel/air charge taken in during the intake stroke. The fuel/air charge varied from being very lean to very rich, with the engine running best over the range from stoichiometric to lean. Although no precise measurements of the RPMs were made as this figure was varying constantly over the range of 450-1600, the best operating conditions appeared to the investigators to coin-

cide with the higher RPM conditions, corresponding to a medium load. Characteristics of the NAHBE cycle were still present under higher load conditions but not as prevalent.

The question then arises as to exactly what is hoped to be uncovered by using high-speed photography as a method of observation. To begin with, it has been previously mentioned in the discussion of the NAHBE cycle that the purpose of the balancing chamber is to reflect the compression shock that goes underneath the pressure exchange cap upon ignition of the fuel/air charge. Before that ignition occurs the composition of the substance in the balancing chamber is directly determined by the fuel-to-air ratio of the fuel/air charge that enters the cylinder during the intake stroke.

Appendix III contains photographs obtained of various operating conditions.

The poisoning of the balancing chamber with fuel rather than air during the intake stroke by admitting a fuel/air charge that was too rich resulted in a break in the chain of events that normally occur in the NAHBE cycle. The high speed photographs clearly show that an overly rich charge allowed some of the fuel to be admitted into the balancing chamber from the combustion chamber. If the resulting fuel/air mixture within the balancing

chamber contained enough fuel ignition of the fuel/air charge in the combustion chamber was followed by the flame propagating across the gap between the balancing and combustion chambers and into the balancing chamber, where there was now enough fuel to permit continuation of the combustion process.

The first result seen of this two-fold combustion is that the NAHBE cycle is broken in that no longer is a compression shock reflected from the balancing chamber without being significantly affected beforehand. During the NAHBE cycle, this shock wave is reflected as a result of the geometry of the pressure exchange cap. When the shock wave first crosses the boundary between the two chambers, the only substance that should be present is the air that entered via the auxiliary air intake. Thus, there should be no further chemical reaction occurring beneath the pressure exchange cap. However, when the mixture beneath the cap contains enough fuel, the flame from the combustion chamber will transit the gap and cause the combustion to continue in the balancing chamber. When this occurs, there is further interaction between the flow that enters the balancing chamber and any shocks that are produced as a result of combustion now taking place below the cap.

On the other hand, the presence of pressure exchange can be seen by the extension of combustion time resulting

from the addition of oxygen to the combustion zone once combustion has been originated. This condition coincided to the lack of significant combustion levels in the balancing chamber when the proper amount of fuel was admitted. When ignition occurs, a high pressure region is present in the combustion chamber and a low pressure region exists in the balancing chamber. For the oxygen in the balancing chamber to be able to transit the gap and enter the combustion chamber, the direction of this pressure differential must be reversed. In order for this to happen, pressure exchange must occur.

As stated previously, pressure exchange is the compression of one medium at the expense of the expansion of another medium. In this case the compression shock wave compresses the medium in the balancing chamber and an expansion wave is reflected in the combustion chamber. The result of this event lowers the pressure in the combustion chamber and increases the pressure in the balancing chamber such that the direction of the pressure differential is now reversed and the oxygen can now transit the gap and enter the combustion chamber. Evidence of this is seen by the presence of blue combustion in the combustion chamber indicating the addition of extra oxygen from the balancing chamber allowing complete combustion to occur. Further supporting evidence of this oscillation of pressures is

seen in the pressure readings shown in Figure 6, discussed previously.

In an effort to minimize the effects of fuel poisoning the balancing chamber, certain alterations may be made to discourage combustion from occurring below the cap. First of all, when the size of the gap (amount of clearance between the pressure exchange cap and cylinder wall) is compared to the size of the molecules present in the environment within the engine, the gap is no longer just a clearance per se, but rather it is a dimension that has a definite effect on what occurs below in the balancing chamber. Decreasing the gap size would allow less fuel to flow into the balancing chamber and help prevent combustion from occurring there. However, flow transitting the gap and entering the balancing chamber "sees" this combination as an increasing-area nozzle and making the gap, or nozzle entrance, too small would restrict the flow of air significantly. This would not only restrict the flow of air into the balancing chamber prior to ignition but also restrict the passage of the wave from the combustion chamber to the balancing chamber and back again after ignition occurs. Consequently, gap size alteration would not be an effective method to discourage combustion below the pressure exchange cap.

Secondly, one parameter not previously discussed that

had an effect on the combustion process was the relative location of the spark plug in the cylinder. On the Megatech Mark III, the spark plug is situated off-center in one dimension. The obvious consequence of such a location is to start the flame propagation off-center. There are some instances where this permitted combustion to occur in the right balancing chamber in the square engine but not in the left balancing chamber. Centering the spark plug would aid in preventing this from happening.

Thirdly, a change in the geometry of the pressure exchange cap so that it is no longer flat on top must be considered. The cap will be "dished" so that the fuel/air charge will tend to concentrate in the center of the cylinder, as shown in Figure 7. By doing this, flame propagation from the center of the cylinder, rather than from some off-center location, will be greatly encouraged.

Another alteration to the geometry of the pressure exchange cap was seen to be necessary from data collected on film during a test run. The formation of a compression shock wave creates a flow in combustion chamber with a Mach number of approximately one. As this flow approaches the gap serving as the interface between the combustion and balancing chambers it sees the gap and balancing chamber as a nozzle, as mentioned beforehand.

The flow undergoes a Prandtl-Meyer expansion upon

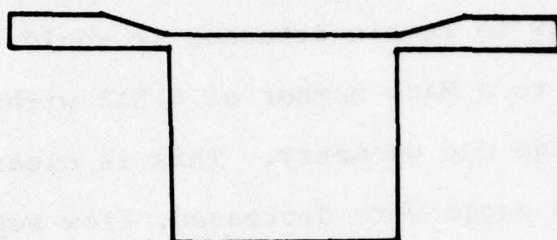


Fig. 7

Pressure Exchange Cap Modification (Top)

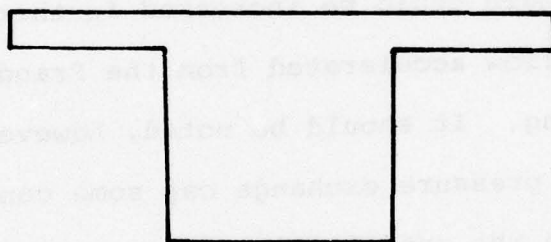


Fig. 8(a)

Pressure Exchange Cap (Unmodified)

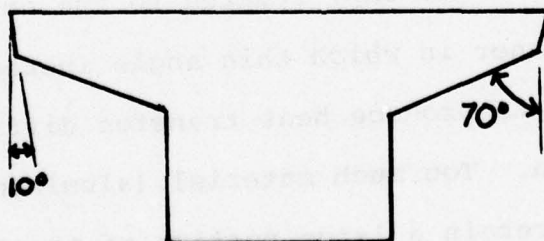


Fig. 8(b)

Pressure Exchange Cap Modification (Balancing Chamber)

passing the corner of the pressure exchange cap. However, the present design has a ninety-degree corner at this interface. For the flow to remain attached it would required to accelerate to a Mach number of 6.819 with present pressure exchange cap geometry. This is clearly impossible, but if this angle were decreased, flow separation could be delayed. Assuming that the flow attains a Mach number of approximately 1.5 upon entering the balancing chamber it would remain attached if the angle at the corner were decreased from 90 to 12 degrees. In a similar fashion the angle could be increased further from 12 degrees as the flow accelerated from the Prandtl-Meyer expansion occurring. It should be noted, however, that in redesigning the pressure exchange cap some concessions must be made in the optimization so as to maintain the previous values of compression and balancing ratios.

Also, the thickness of the cap, related to the angle at the corner and the manner in which this angle increases, must not be too great as to produce heat transfer difficulties during combustion. Too much material (aluminum) in the cap causes it to retain a large portion of the heat liberated during combustion and will adversely affect engine performance.

A water flow table study was conducted to determine what effects various geometry changes to the cap have on the quality of the flow underneath the cap (in the balancing chamber). The alteration depicted in Figure 8(b) involves decreasing the corner angle from 90 degrees to 10 degrees. The angle is increased to 70 degrees after the critical distance around the corner has passed. Flow studies indicated a significant delay in flow separation from the cap as compared to the separation occurring using the existing cap design, shown in Figure 8(a). As noted previously, this modification is necessarily not the optimum case. However, the combination of the changes in Figures 7 and 8(b) permits efficient heat transfer to continue and maintains the balancing and compression ratios at the values prior to any cap alterations.

The end result of the proposed modifications to cap geometry will be two-fold. First, poisoning of the balancing chamber by fuel will be discouraged by altering the top of the pressure exchange cap. This will permit the NAHBE cycle to exist under all fuel-to-air ratios of the fuel-air charge entering during intake stroke. Second, geometry changes to the cap within the balancing chamber will permit greater interaction between the flow from the combustion chamber and the oxygen forced under the cap during the compression stroke. This supplies more oxygen

to the combustion chamber as the shock wave is reflected back from the balancing chamber. Moreover, this process is made more efficient by decreasing the turbulence level beneath the pressure exchange cap. The consequence of enhancing the NAHBE cycle through these modifications will be an associated increase in engine performance. In concise terms, that is the purpose of this study of NAHBE combustion.

IV. FUTURE WORK

For future experiments, more sophisticated optical methods will be used for analyzing the combustion in the NAHBE engine. Color Schlieren and holographic interferometry will be employed. Techniques such as these will permit detailed wave analysis and result in a more thorough understanding of the combustion processes in the NAHBE cycle.

REFERENCES

1. Blaser, R. F., The Heat Balanced Cycle, Mechanical Engineering Master's Paper, University of Maryland, 1974.
2. Blaser, R. F., Pouring, A. A., Keating, E. L., and Rankin, B. H., The Naval Academy Heat Balanced Engine (NAHBE), USNA Report EW#8-76, June 1976.
3. Foa, J. V., Elements of Flight Propulsion, John Wiley, New York, 1960.
4. Rudinger, G., Wave Diagrams for Nonsteady Flow, Van Nostrand, New York, 1955.
5. Pouring, A. A., Blaser, R. F., Keating, E. L, and Rankin, B. H. The Influence of Combustion with Pressure Exchange on the Performance of Heat Balanced Combustion Engines, SAE Report #770120, March 1977.

APPENDIX I

DRAWINGS

No.	Title	Revision
1	Cylinder Arrangement	2
2	Crosshead Case Pc #6, 21, 25	5
3	Same	2
4	Cylinder Head Pc #15	3
5	Cylinder Clamps Arrangement	0
6	Cylinder Clamps Pc #18, 19, 20	0
7	Crosshead Pc #7	1
8	Cylinder Pins Pc #1, 2, 3	1
9	Connecting Rod Parts Pc #8, 9, 10	2
10	Piston Arrangement	1
11	Piston Pc #11, 27	0
12	Piston Ring Arrangement	0
13	Piston Ring Details Pc #17, 30	0
14	Piston Guides Details Pc #16, 28, 29	1
15	Pressure Exchange Cap Pc #26	0

Fig. I-1

Drawings

Pc #	Description	No.	Material	Drawing #		Completion Status			
				Arr'y't.	Detail	Drug %	Material	Mfg %	Remarks
1	Cylinder Glass	2	Pyrex, Vloor	1	8	100			Megatech ltr.
2	Cylinder Slide	2	Alum, Inver	1	8	100			Megatech ltr.
3	Cylinder Wedge	2	Alum, Inver	1	8	100			Megatech ltr.
4	Cylinder Top Gasket	1	1/16" Teflon TFE	-	4	100			Megatech ltr.
5	Cylinder Bottom Gasket	1	1/16" Teflon TFE	-	3	100			Megatech ltr.
6	Crosshead Case	1	Alum.	-	2,3	100	stock		
7	Crosshead	1	Steel	2	7	100	stock		
8	Upper Connecting Rod	1	Alum	10	9	90	stock		
9	Upper Connecting Rod Pins	2	Steel	10	9	100	stock		
10	VCR Pin Spacers	4	Teflon	10	9	100			Mag. ltr.
11	Piston	1	Alum	10	11	100	stock		
*12	Lower Conn Rod (Existing)	1	Alum	-	-	-	old eng.	90	
*13	Lower Conn Rod Pin	1	Steel	-	-	-	old eng.	100	
*14	Lower Conn Rod Pin Spacers	2	Teflon	-	-	-	old eng.	100	
*15	Cylinder Head (modify)	1	Alum.	-	4	100	old eng.		
16	Upper Piston Guide	1	Carbon	10	14	100			Mag. ltr.
17	Piston Ring Segments	12	Teflon	12	13	100			Mag. ltr.
18	Cylinder Clamp #1	2	Alum.	5	6	100	stock		
19	Cylinder Clamp #2	1	Alum.	5	6	100	stock		
20	Cylinder Clamp #3	1	Alum.	6	6	100	stock		
*21	Crosshead Bearing	1	-	-	2	100	-	ordered	
22	Kistler Gage (w access)	2	-	10	-	100	-		
23	Gage Bushing	2	Brass	10	-	100	stock		
24	Retaining Ring	6	Steel	10	-	100	-	ordered	TruArc N8000-22
25	Retaining Ring	1	Steel	2	-	100	-	ordered	TruArc 8000-237
26	Pressure Exchange Cap	1	Alum.	10	15	100	stock		
27	Lower Piston Guide Retainer	1	Alum.	-	11	100	stock		
28	Lower Piston Guide		Carbon	-	14	100			
29	Upper Piston Guide Stud	1	Steel	-	14	100	stock		
*30	Piston Ring Expander	12	Silicone Rubber	12	13	100			
31	Cylinder Head Bolts	4	Steel	-	5	100	stock		

Fig. I-2 Material List

RTV adhesive GE type 106

SECTION AA'

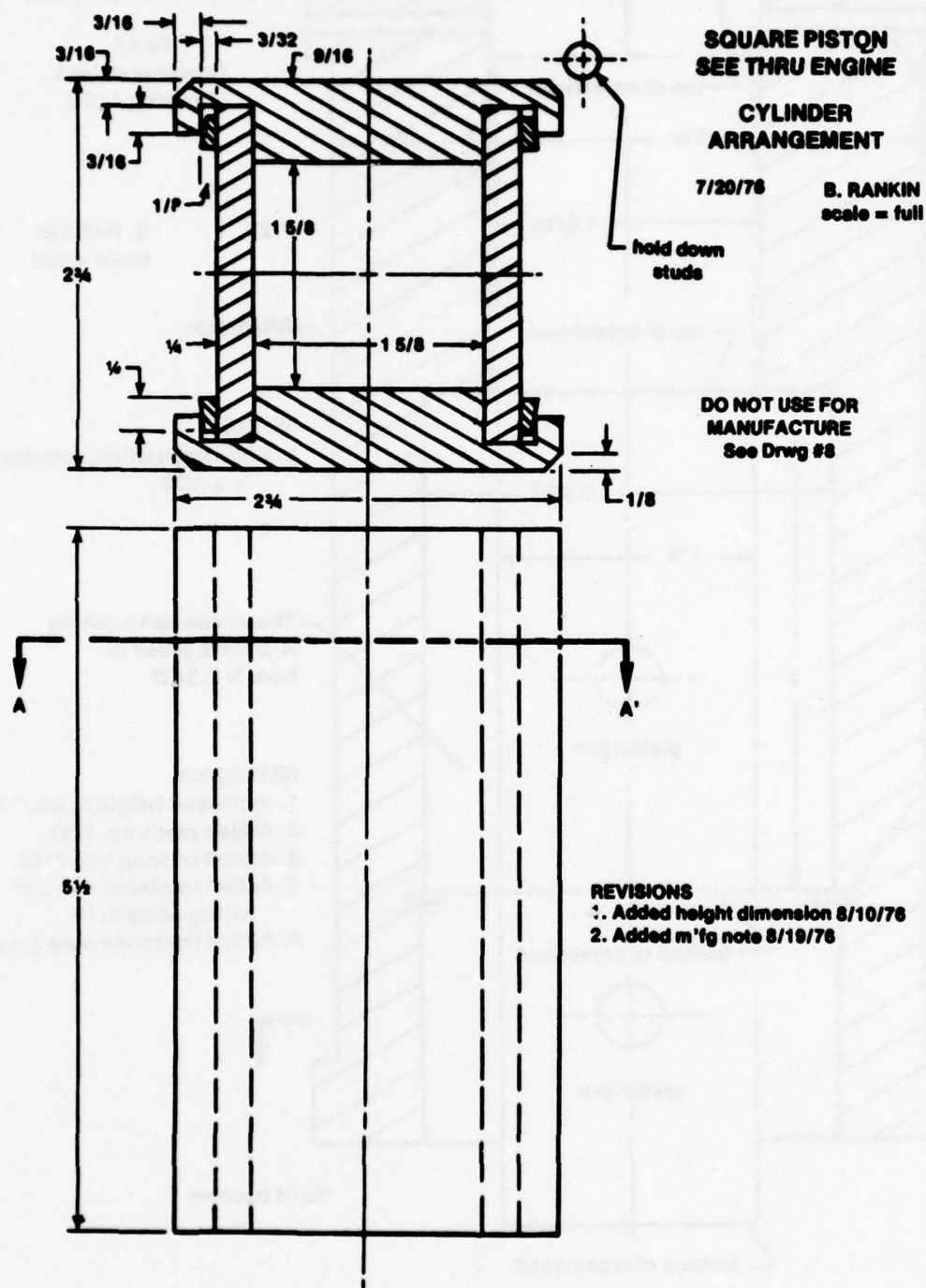


Fig. I-3

Cylinder Arrangement

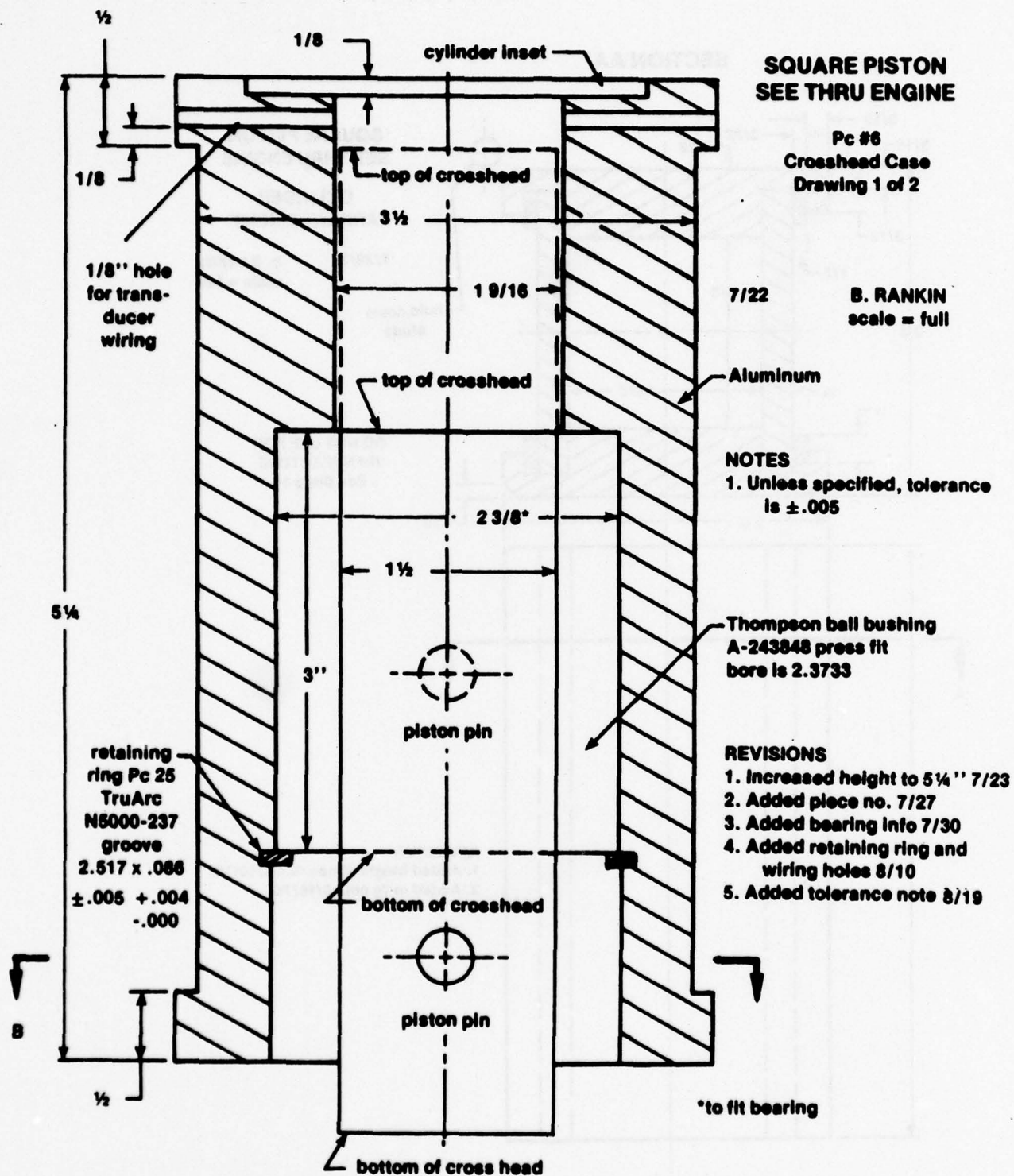


Fig. I-4 Crosshead Case Pc #6

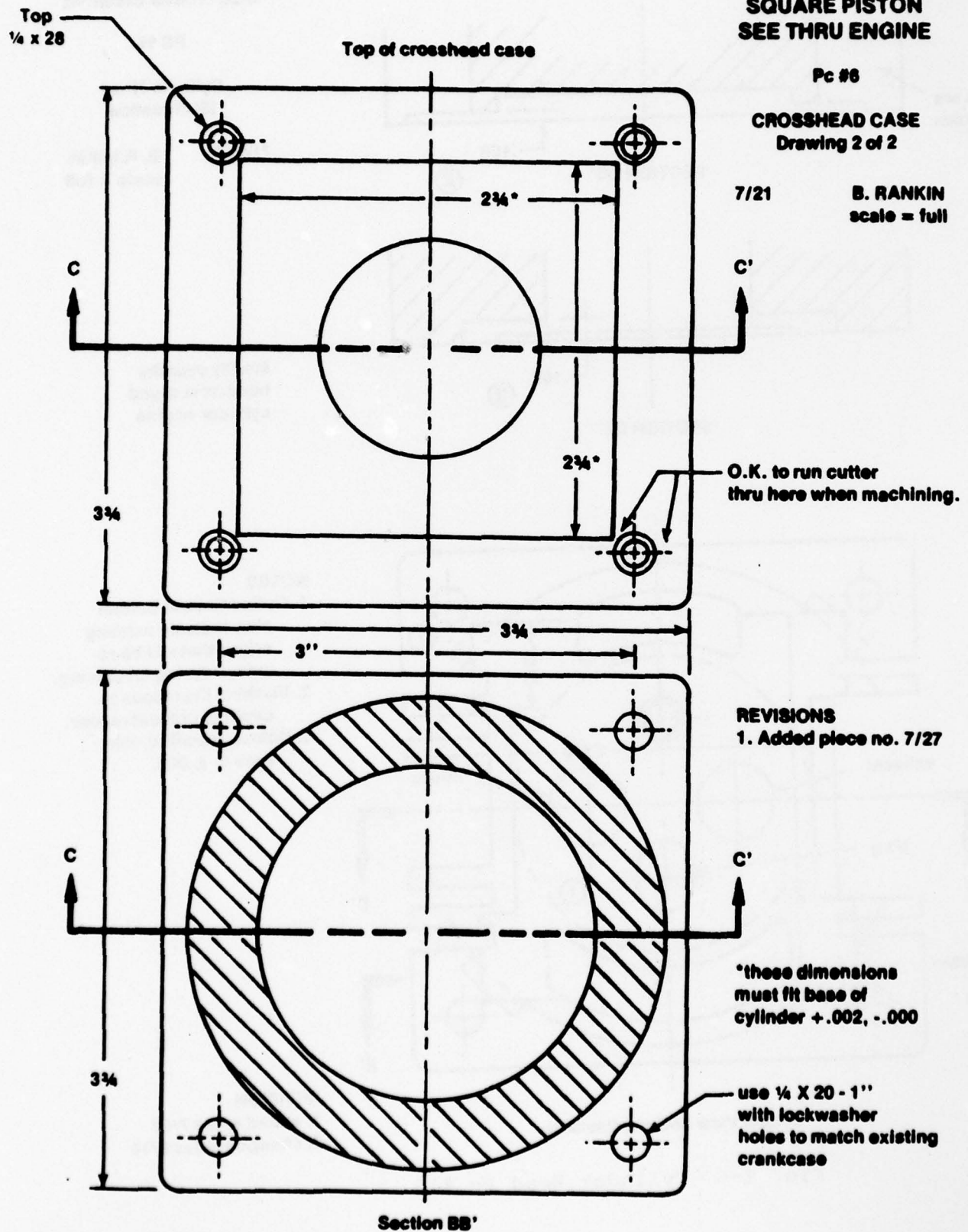


Fig. I-5 Crosshead Case Pc #6

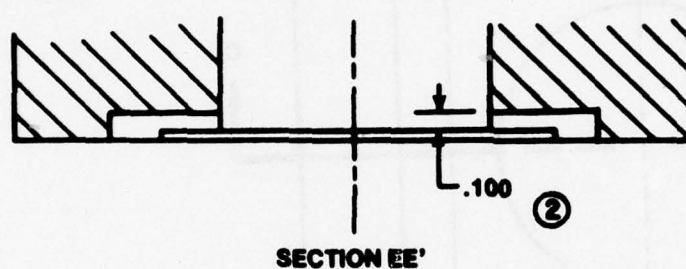
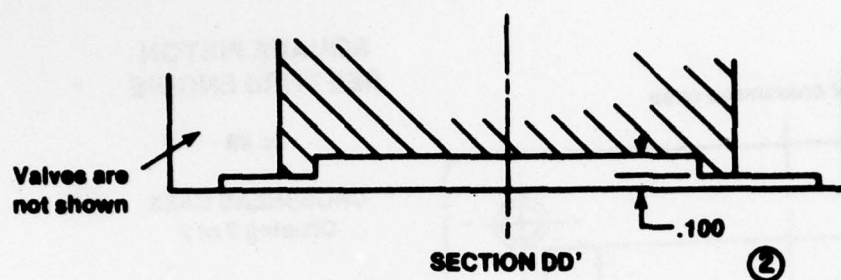
SQUARE PISTON SEE-THRU ENGINE

PC 15

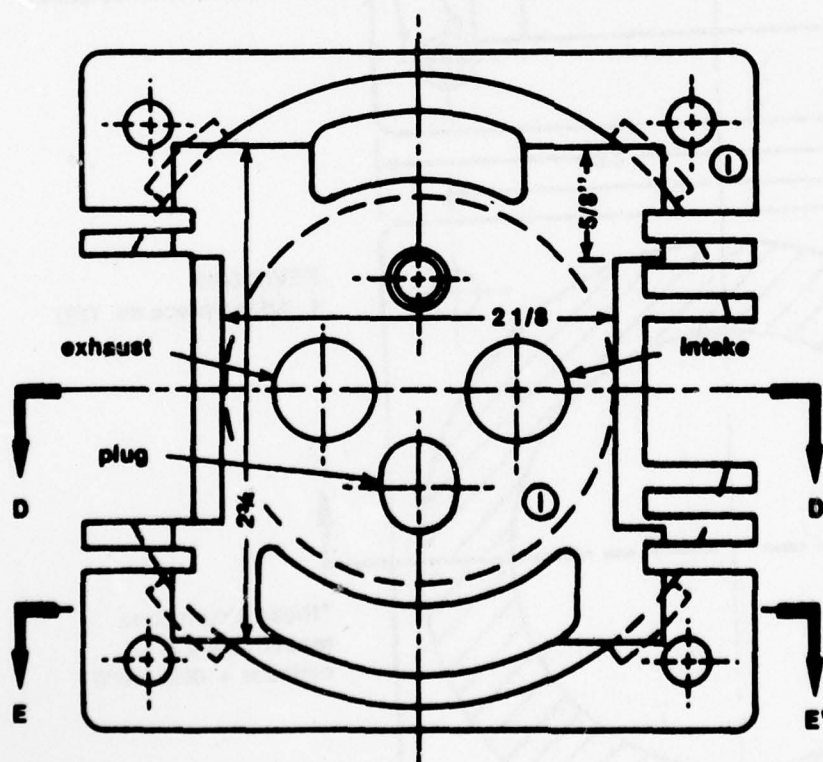
**Cylinder Head
Modification**

7/25/76

**B. RANKIN
scale = full**



**Modify cylinder
head from round
cylinder engine**



NOTES

1. Dotted lines in bottom view indicate existing edges that will be removed during machining.
2. Machine the recess to depth of present recess.
3. Unless specified, tolerance is $\pm .005$.

REVISION

1. added notes 7/28
2. changed notes 8/19

Fig. I-6 Cylinder Head Pc #15

SQUARE PISTON SEE-THRU ENGINE

**CYLINDER
ARRANGEMENTS
Pc #18, 19, 20, 31**

7/19/76

B. H. RANKIN
scale = full
part NTS

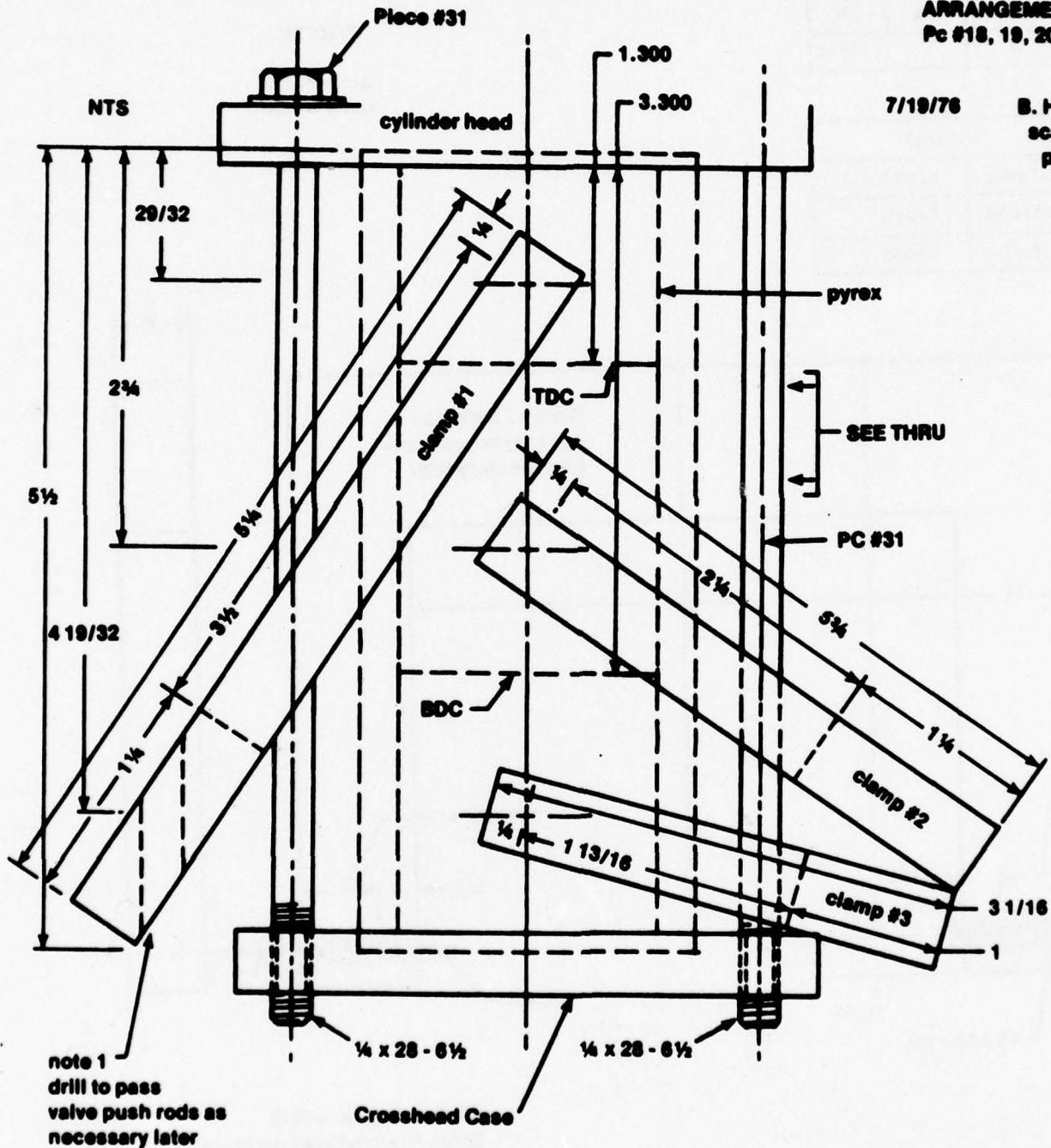


Fig. I-7 Cylinder Arrangements Pc# 18,19,20,31

REVISIONS

1. changed clamp #1
added note 1 7/21
2. added vertical dimensions 8/10
3. added Pc #31 8/20

SQUARE PISTON SEE-THRU ENGINE

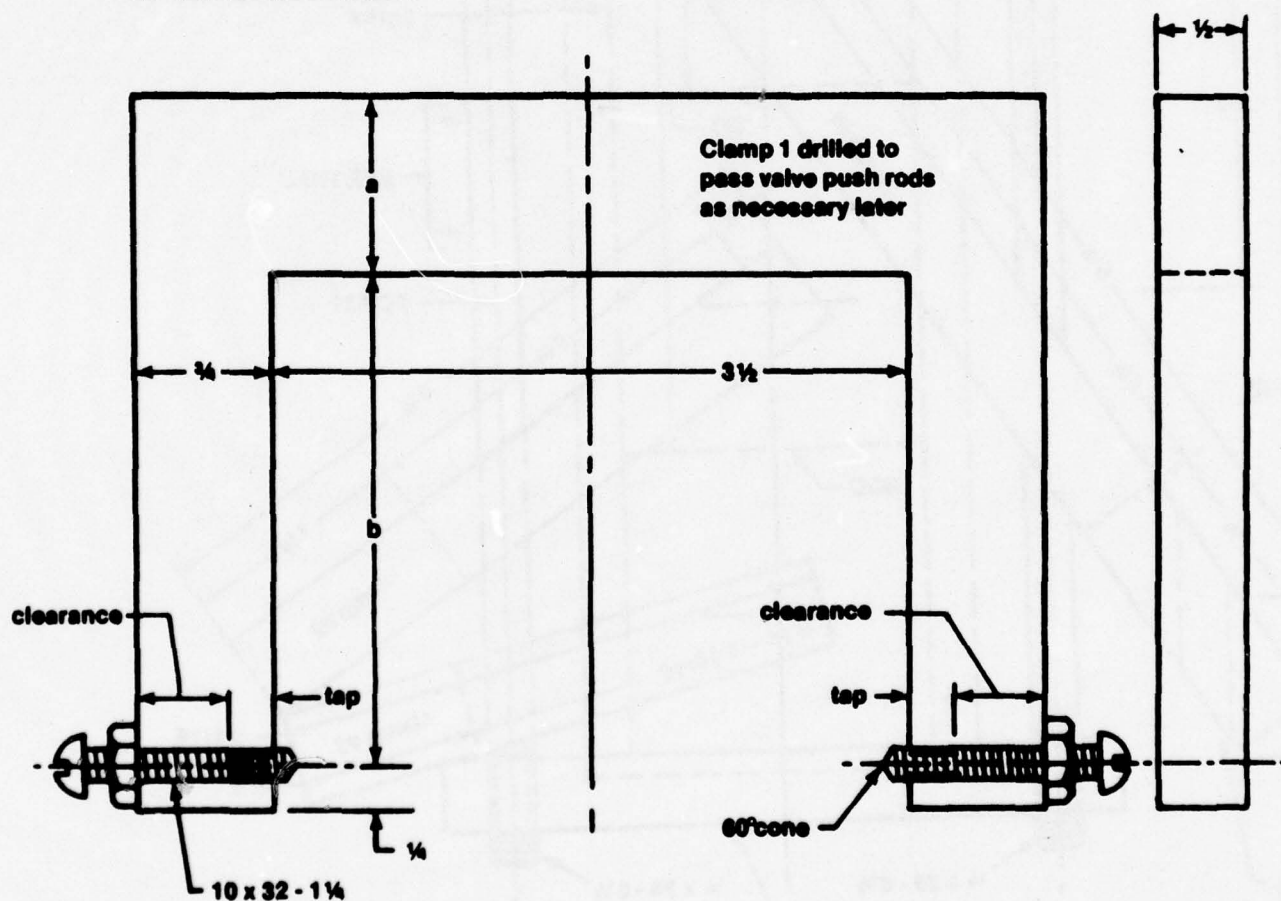
CLAMP DETAILS Pc #18, 19 20

7/20/76

B. RANKIN
scale = full

Clamp	Dimensions	
	a	b
1	1½	3½
2	1¼	2¼
3	1	1 13/16

material	
clamp	aluminum
screws	brass
nuts	brass



All dimensions $\pm .010$
Break sharp edges—no burrs

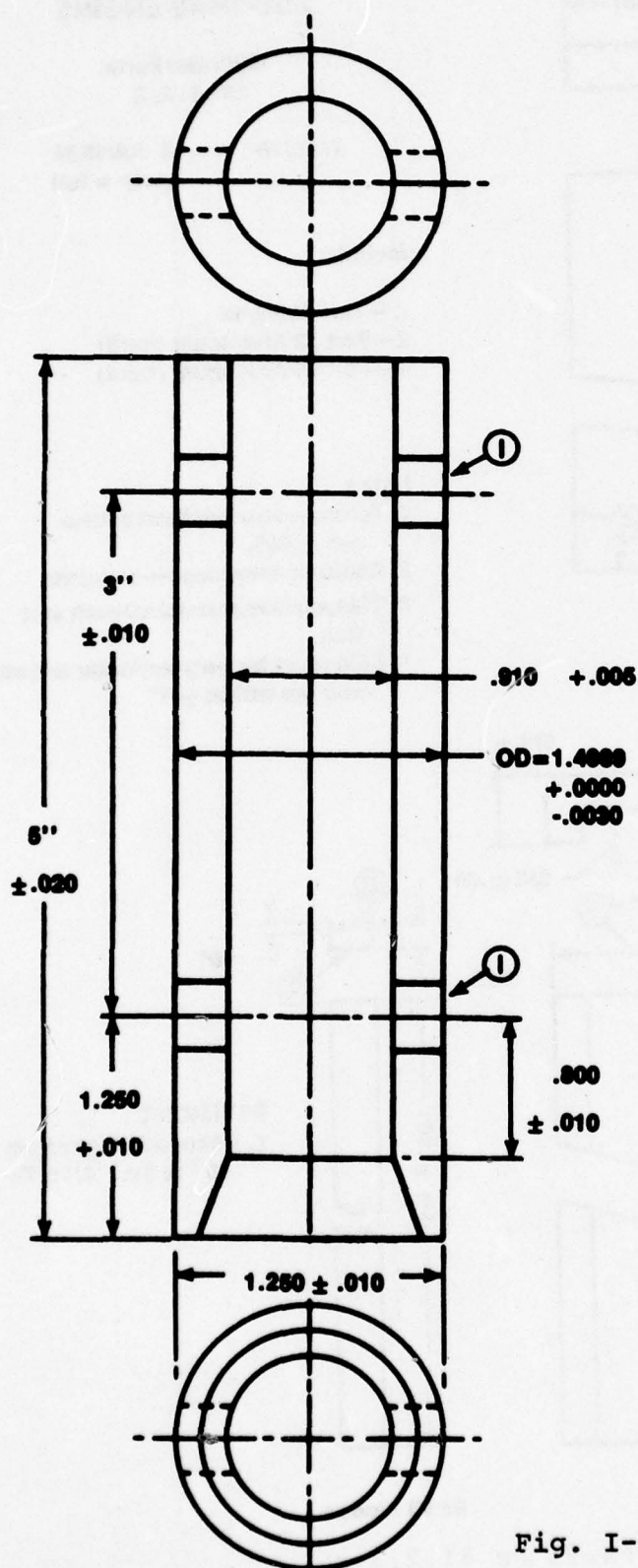
Fig. I-8 Cylinder Clamps Pc#18,19,20

SQUARE PISTON SEE-THRU ENGINE

**CROSS HEAD
Pc 7**

7/16/76

B. H. RANKIN
full scale



NOTES:

1. Piston pin hole .3745-.3740" diam thru both walls. Hole to be on centerline within $\pm .003$ " and perpendicular to centerline of piston to $\pm .5^\circ$

Break sharp edges—no burrs

REVISIONS

1. Added upper piston pin
Changed notes 7/28

Fig. I-9 Crosshead Pc #7

SQUARE PISTON SEE-THRU ENGINE

Cylinder Parts
Pc 1, 2, 3

7/27/76

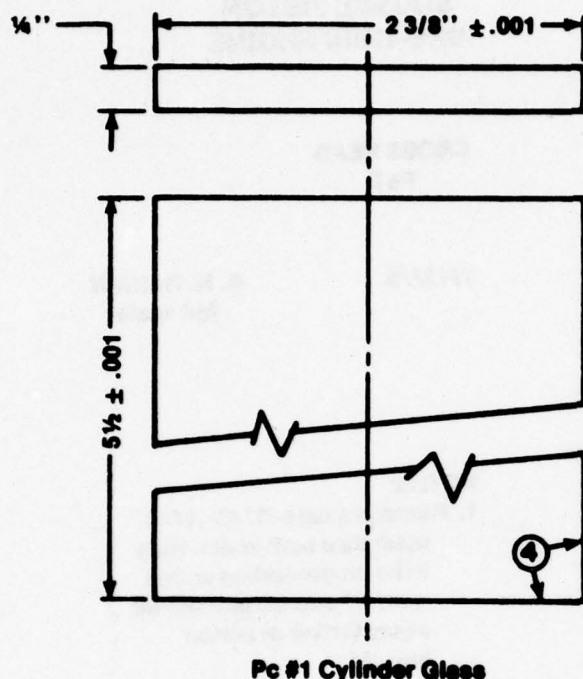
B. RANKIN
scale = full

Material

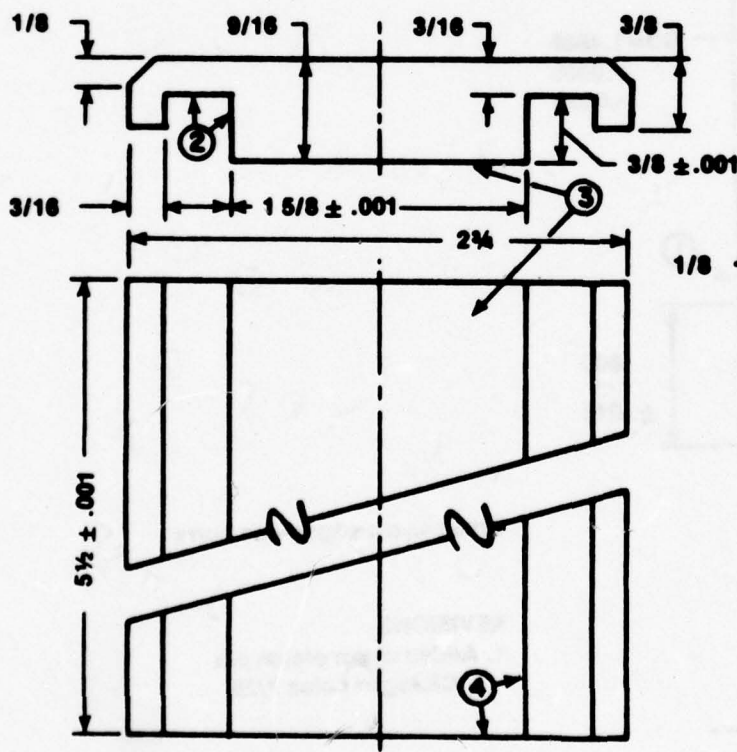
2— Part #1 Pyrex
2—Part #2 Aluminum (hard)
4—Part #3 Aluminum (hard)

Notes

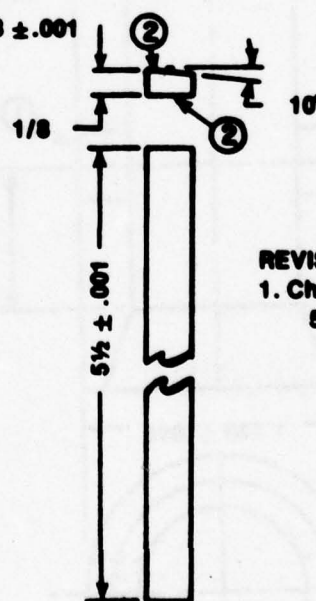
1. Tolerances other than shown are $\pm .005$
2. Surfaces very clean—no burrs
3. This surface ground smooth and flat.
4. Side must be perpendicular to bottom and top within $\pm .1^\circ$



Pc #1 Cylinder Glass



Pc #2 Cylinder Side



Pc #3 Wedge

REVISIONS

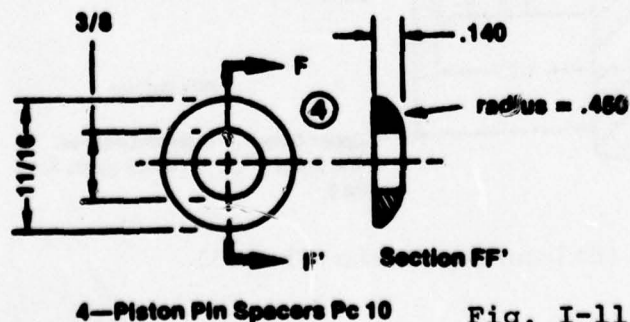
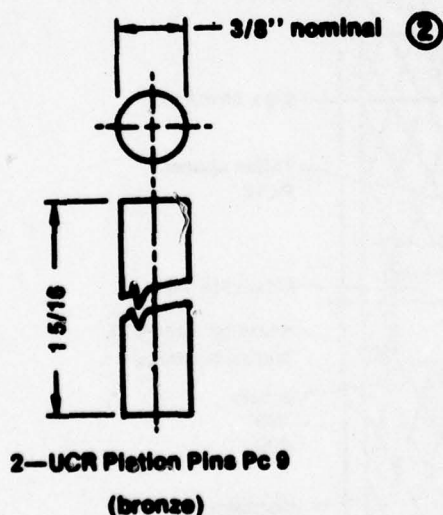
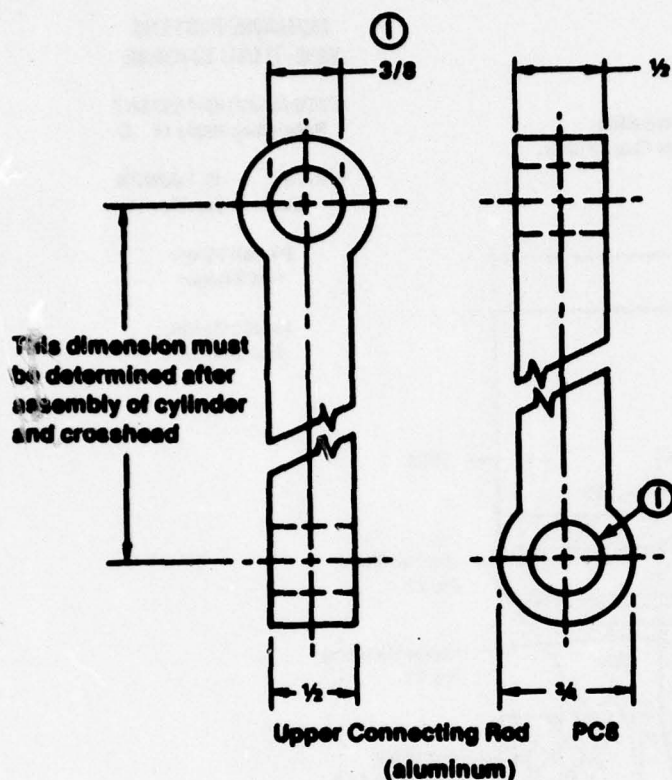
1. Changed height from 5" to 5 1/2" 8/10/76

Fig. I-10 Cylinder Parts Pc #1,2,3

SQUARE PISTON SEE-THRU ENGINE

Upper Connecting Rod
&
UCR Piston Pins
&
UCR Piston Pin Spacers

7/28 B. RANKIN



NOTES

1. Piston pins in upper connecting rod use no bearing. Provide clearance for grease.
2. Piston pins in piston and in crosshead is finger push fit.
3. All dimensions $\pm .010$ unless specified otherwise.
4. All dimensions on spacers $\pm .005$

REVISIONS

1. Changed radius Pc 9 8/3/78
2. Added conn. rod length note 8/20/78

Fig. I-11 Connecting Rod Parts

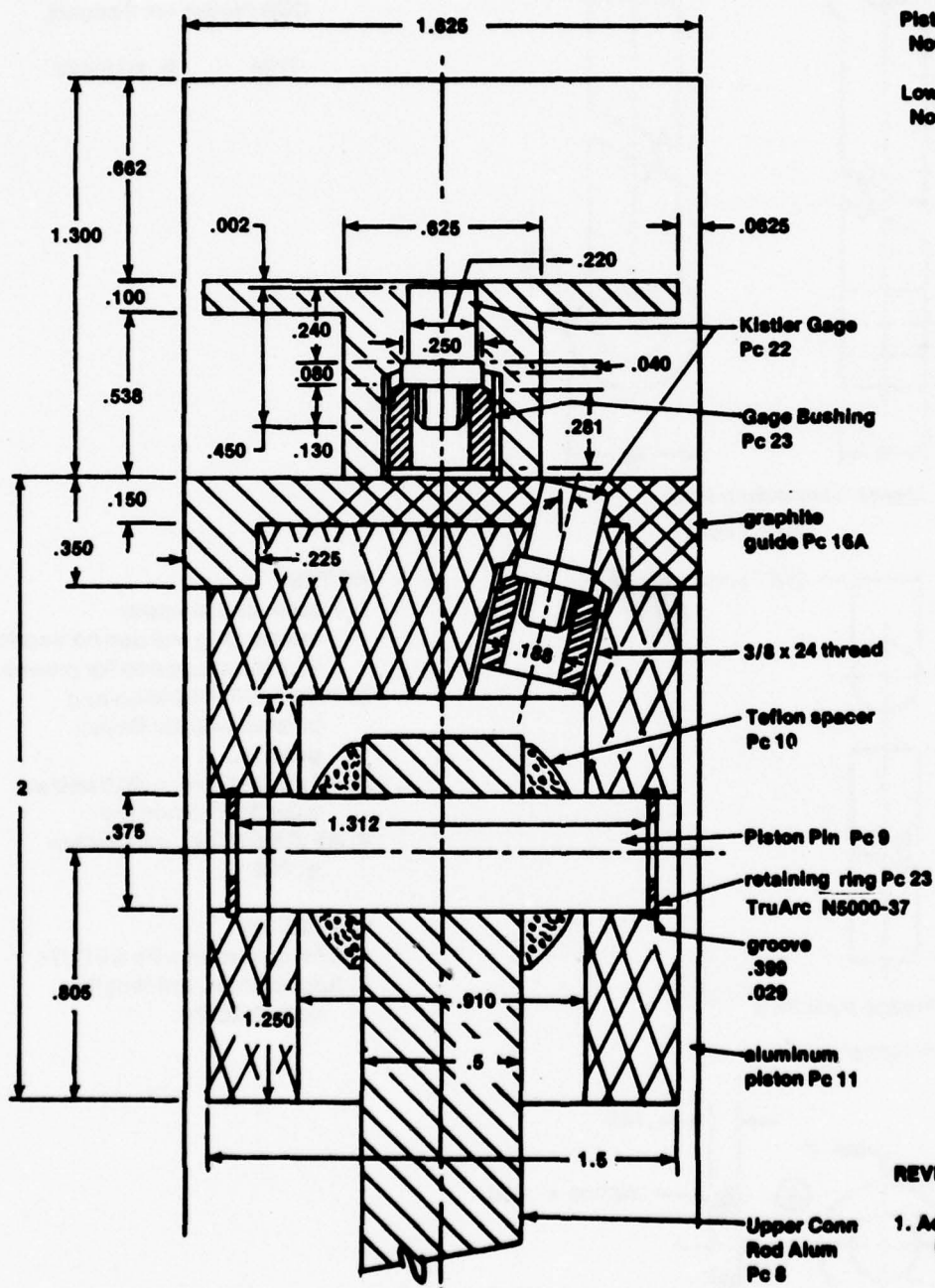
SQUARE PISTON SEE-THRU ENGINE

**PISTON ARRANGEMENT
Balancing Ratio of .5**

**8/6/76 B. RANKIN
scale = double**

**Piston Rings
Not Shown**

**Lower Guide
Not Shown**



REVISIONS

1. Added note on lower guide 8/19

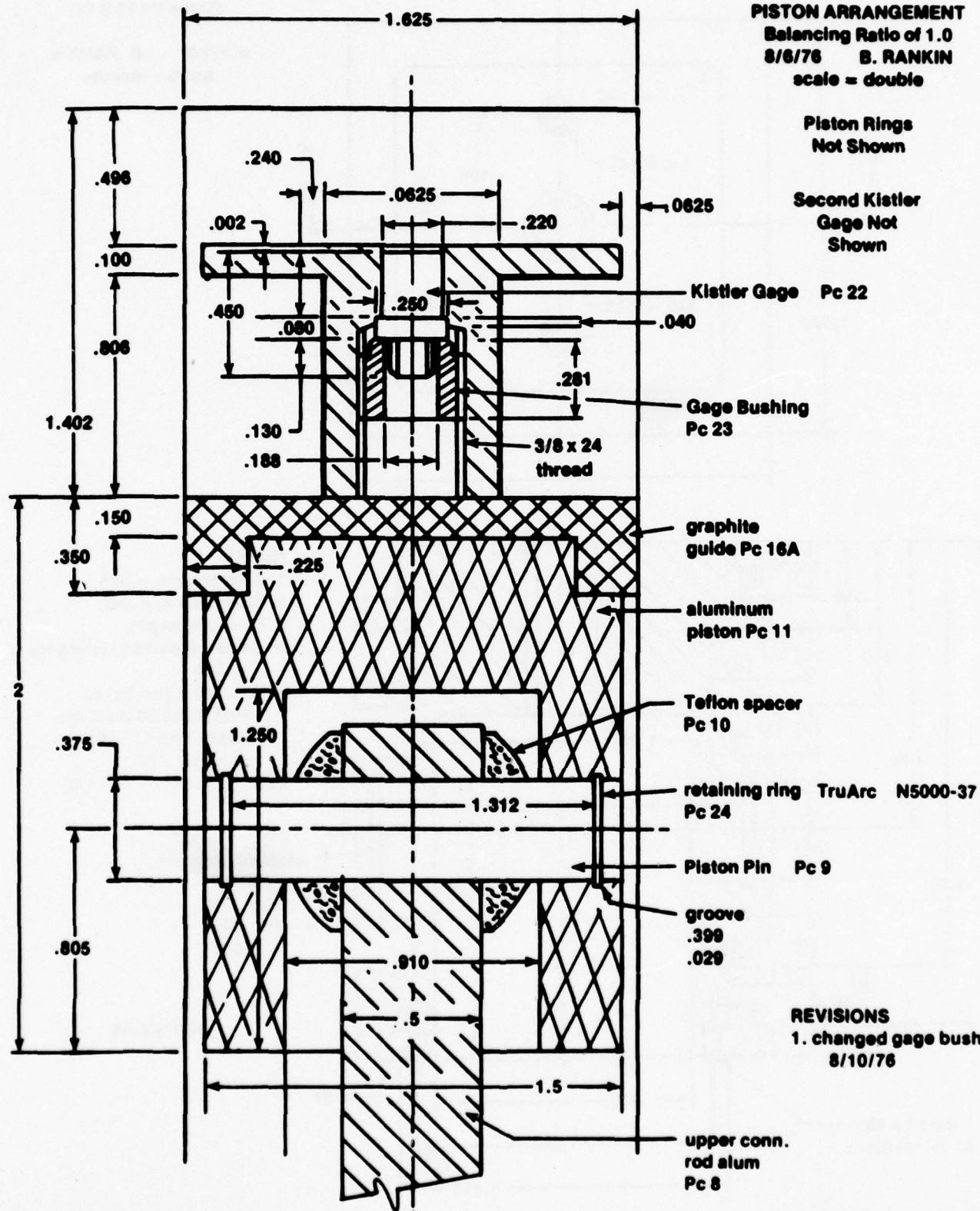
Fig. I-12 Piston Arrangement (Balancing Ratio of 0.5)

SQUARE PISTON SEE-THRU ENGINE

PISTON ARRANGEMENT
Balancing Ratio of 1.0
8/6/76 B. RANKIN
scale = double

Piston Rings
Not Shown

Second Kistler
Gage Not
Shown



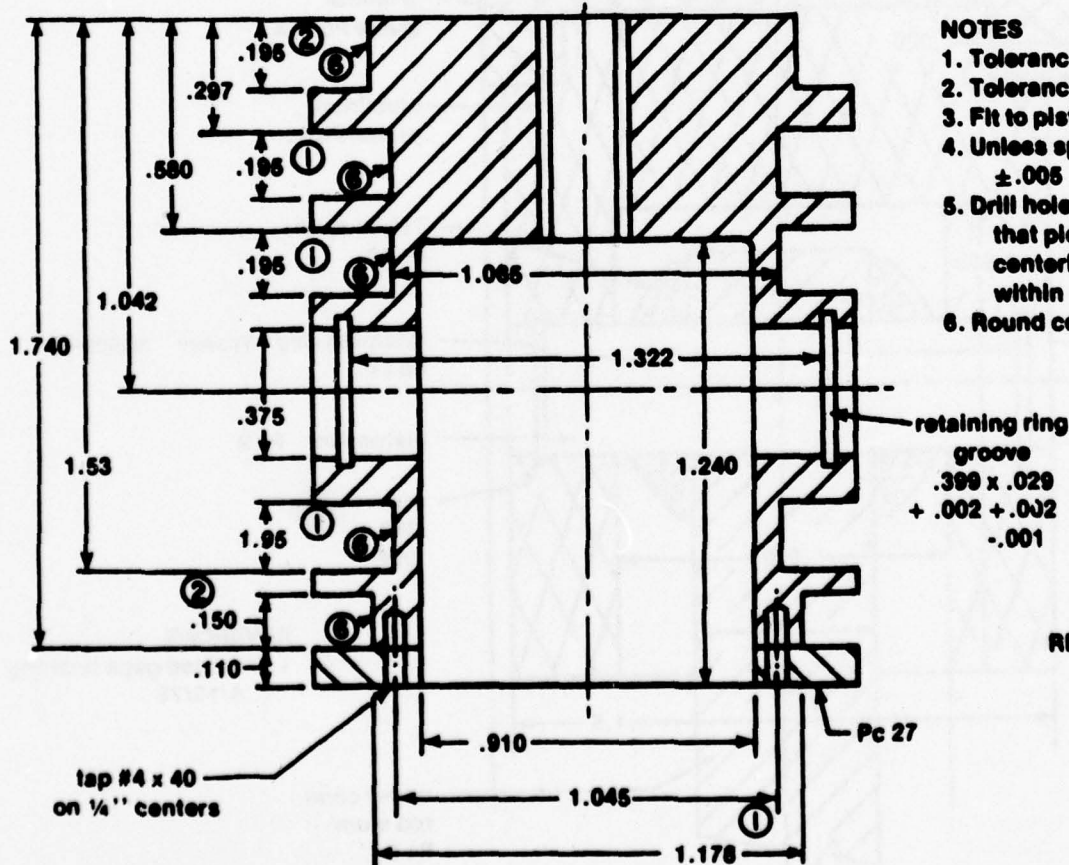
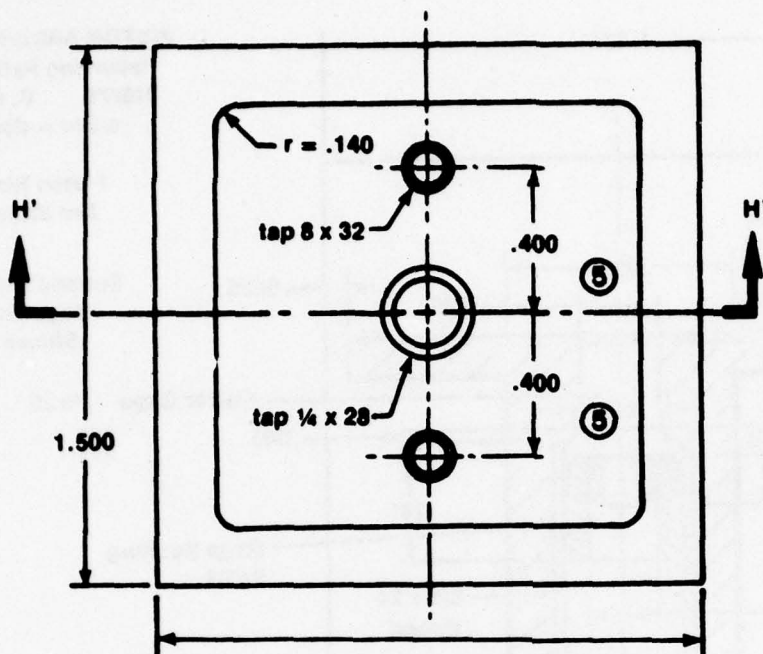
REVISIONS
1. changed gage bushing
8/10/76

Fig. I-13 Piston Arrangement (Balancing Ratio of 1.0)

SQUARE PISTON SEE-THRU ENGINE

Piston Pc 11 & 27

8/17/76 B. RANKIN
scale = double

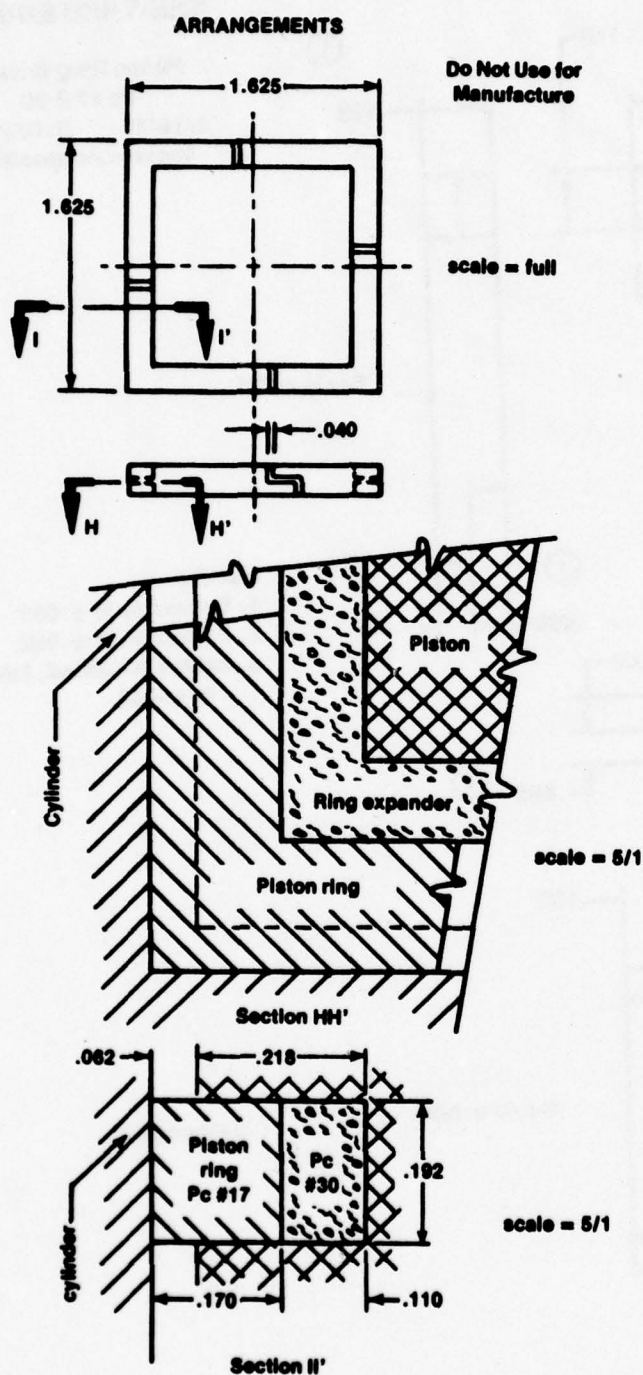


NOTES

1. Tolerance is $\pm .001$
2. Tolerance is $\pm .002$
3. Fit to piston pin
4. Unless specified, tolerance is $\pm .005$
5. Drill holes and tap so that piece 26 matches centerline with piece 11 within $\pm .002$
6. Round corners $r = .140$

REVISIONS

Section HH' Fig. I-14 Piston Pc #11,27



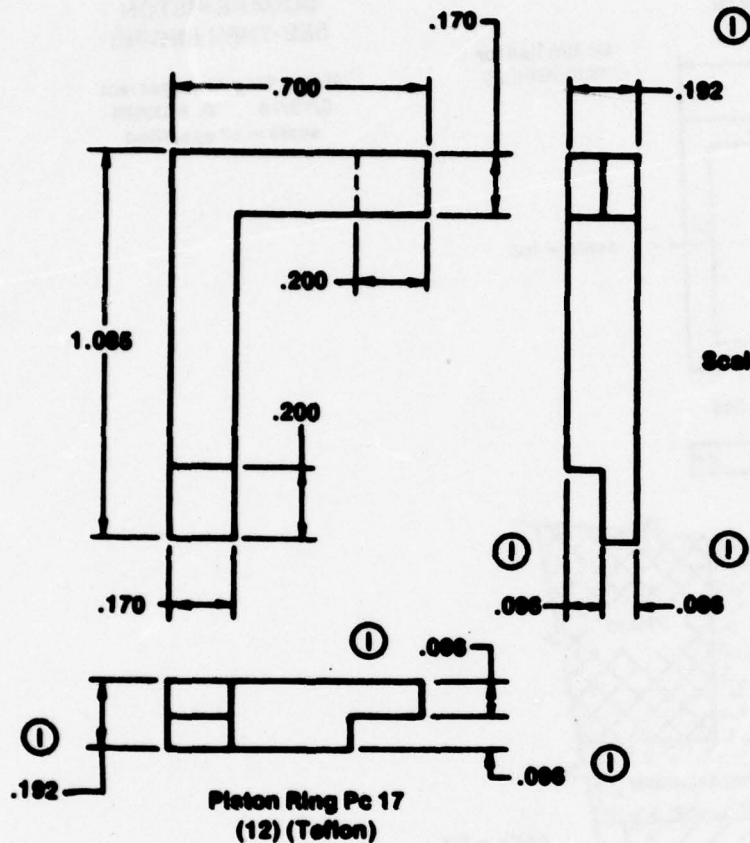
SQUARE PISTON SEE-THRU ENGINE

Piston Ring Arrangement
8/19/76 B. RANKIN
scale = as specified

REVISIONS

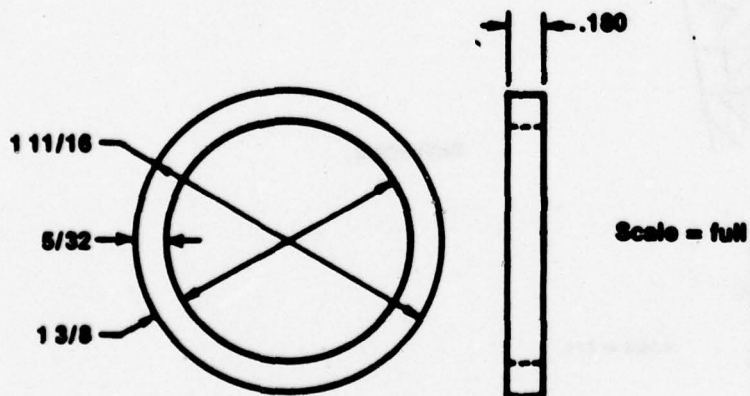
Fig. I-15 Piston Ring Arrangement

DETAILS

SQUARE PISTON
SEE-THRU ENGINEPiston Ring Details
Pc 17 & 308/19/76 B. RANKIN
scale = as specified

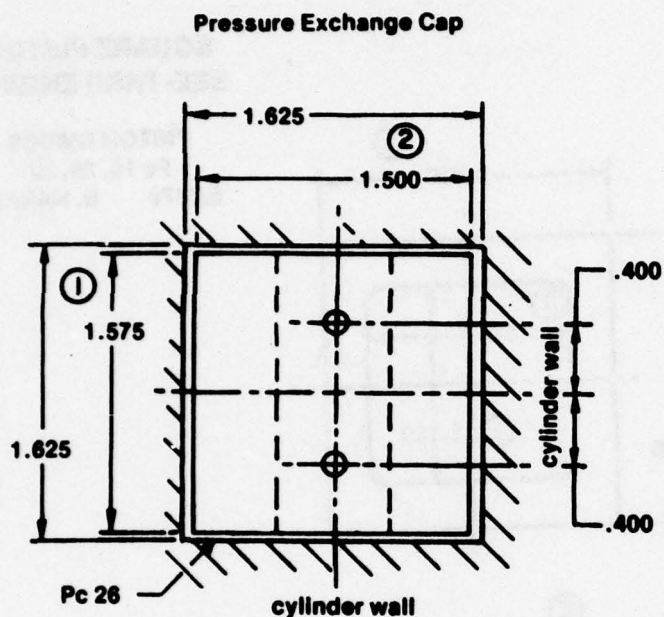
NOTES:

1. Tolerance is $\pm .001$
2. Tolerance is $\pm .002$
3. Unless specified, tolerance is $\pm .005$

Ring Expander Pc 30
(3) (Silicone Sponge Rbr.)

REVISIONS

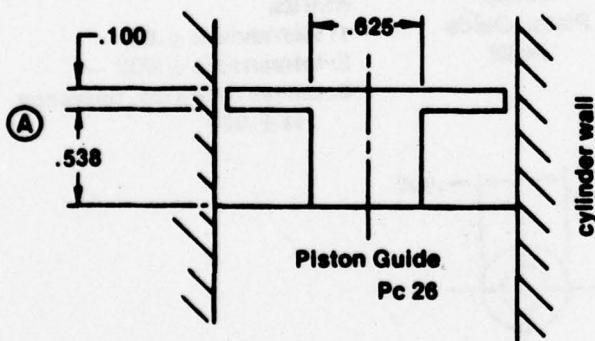
Fig. I-16 Piston Ring Details Pc #17,30



**SQUARE PISTON
SEE-THRU ENGINE**

Pressure Exchange Cap
Pc 26

8/20/76 B. RANKIN
scale = full



- Ⓐ Balancing Ratio**
For balancing ratio of
.5 use .538
1.0 use .806

NOTES

1. Tolerance is $\pm .001$
2. Tolerance is $\pm .002$
3. Drill holes for 8 x 32 machine screws so that Pc 86 and Pc 11 match center
4. Unless specified, tolerance is $\pm .005$

REVISIONS

Fig. I-18 Pressure Exchange Cap Pc #26

APPENDIX II

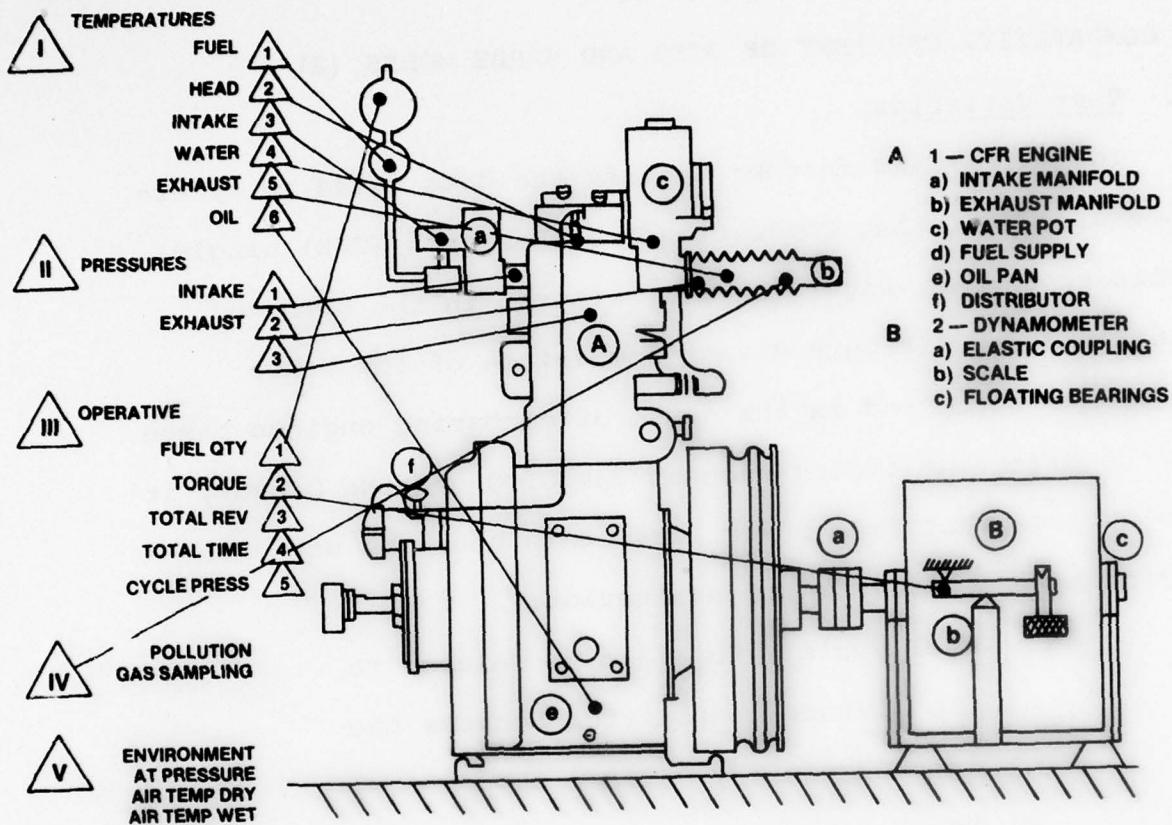
COMPARATIVE CFR TEST OF OTTO AND NAHBE MODES (2)

1. Test Variables

To confirm and further amplify the data cited in reference 3, an existing Combustion Fuel Research (CFR) single-cylinder engine, Figure II-1.1, was run in the OTTO and NAHBE modes. Although direct comparison of the Nahbe should be conducted in the sense of comparing engines based on the different cycles such as the OTTO and the Diesel, it was decided that five basic parameters could be used for performance comparison and evaluation:

- o Fuel cycle: This can be related to the mixture composition because the intake geometry was not changed.
- o Total output: THP (or IHP), where brake plus internal frictional output, equals total output, assuming equal heat losses.
- o Brake output
- o Specific fuel consumption: Using fuel per total horsepower hour, noting that in the single-cylinder CFR engine internal friction is greater than brake output.
- o RPM: Revolutions per minute

VARIABLES



INSTRUMENTATION

I TEMPERATURES

SENSOR—IRON CONSTANTAN THERMOCOUPLES
READOUT—SOLID STATE DIGITAL THERMOMETER

II PRESSURES

SENSOR AND READOUT—MERCURY COLUMNS

III OPERATIVE

- 1 CALIBRATED CONTAINER 50cc
 - 2 SCALE
 - 3 PULSE COUNTER
 - 4 ELECTRICAL STOPWATCH
 - 5 SENSOR—QUARTZ TRANSDUCER WITH SIGNAL CONDITIONER
- POSITION — ANGULAR SIGNAL
READING — OSCILLOSCOPE FOR DIAGRAM AND PEAK PRESSURE
RECORDING — PEAK PRESSURES

Fig. II-1.1
CFR engine details

2. Basic Test Procedures, Open Throttle Configuration

Test Procedures: The CFR engine in its full open throttle configuration was operated in the OTTO and NAHBE modes at 900, 1100, 1200, 1300, and 1500 rpm. Data were recorded at five output loads at each rpm cited within the operational range of each engine mode. A second series of tests was also performed by optimizing the engines for best economy at each rpm, both fuel/air ratio and spark advance were varied for the OTTO and timing only in the NAHBE.

3. Test Results, Open Throttle Configuration

a) Peak Pressure:

Figure II-3.1, the peak pressure at maximum load of the NAHBE mode is 40% or less than that of the OTTO mode. Because the NAHBE maintains high volumetric efficiency and subsequently high cylinder pressure at the point of ignition, the engine also operates satisfactorily at lower loads and rpm than the OTTO. As is shown later the NAHBE will operate at very low rpm with or without a load.

b) Exhaust Temperature:

The results of Figure II-3.2 demonstrate one of the outstanding features of the NAHBE. A well-known characteristic of the OTTO leads to exhaust valve damage: this is because, as the mixture is reduced below that of

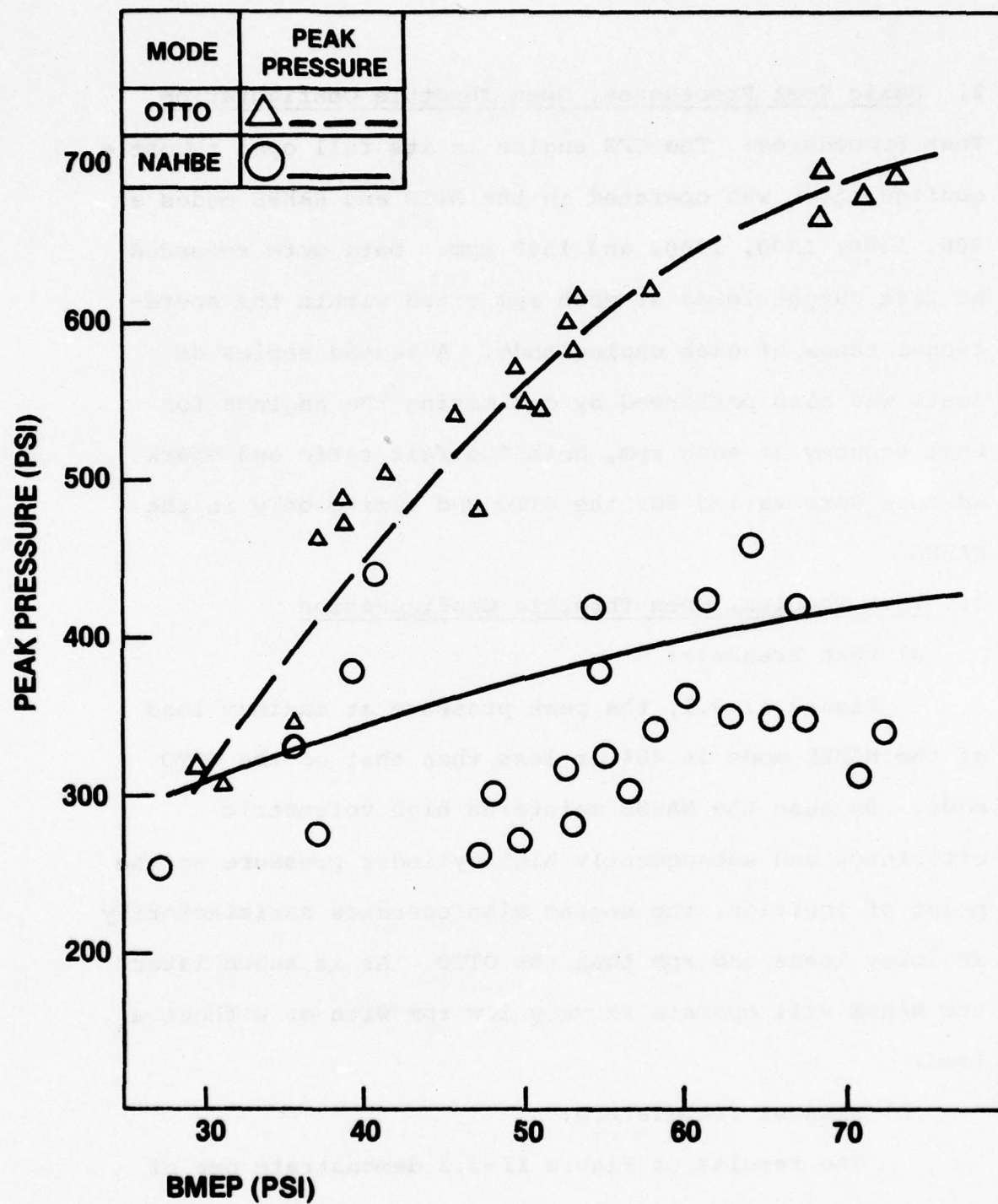


Fig. II-3.1
CFR comparison of peak pressures

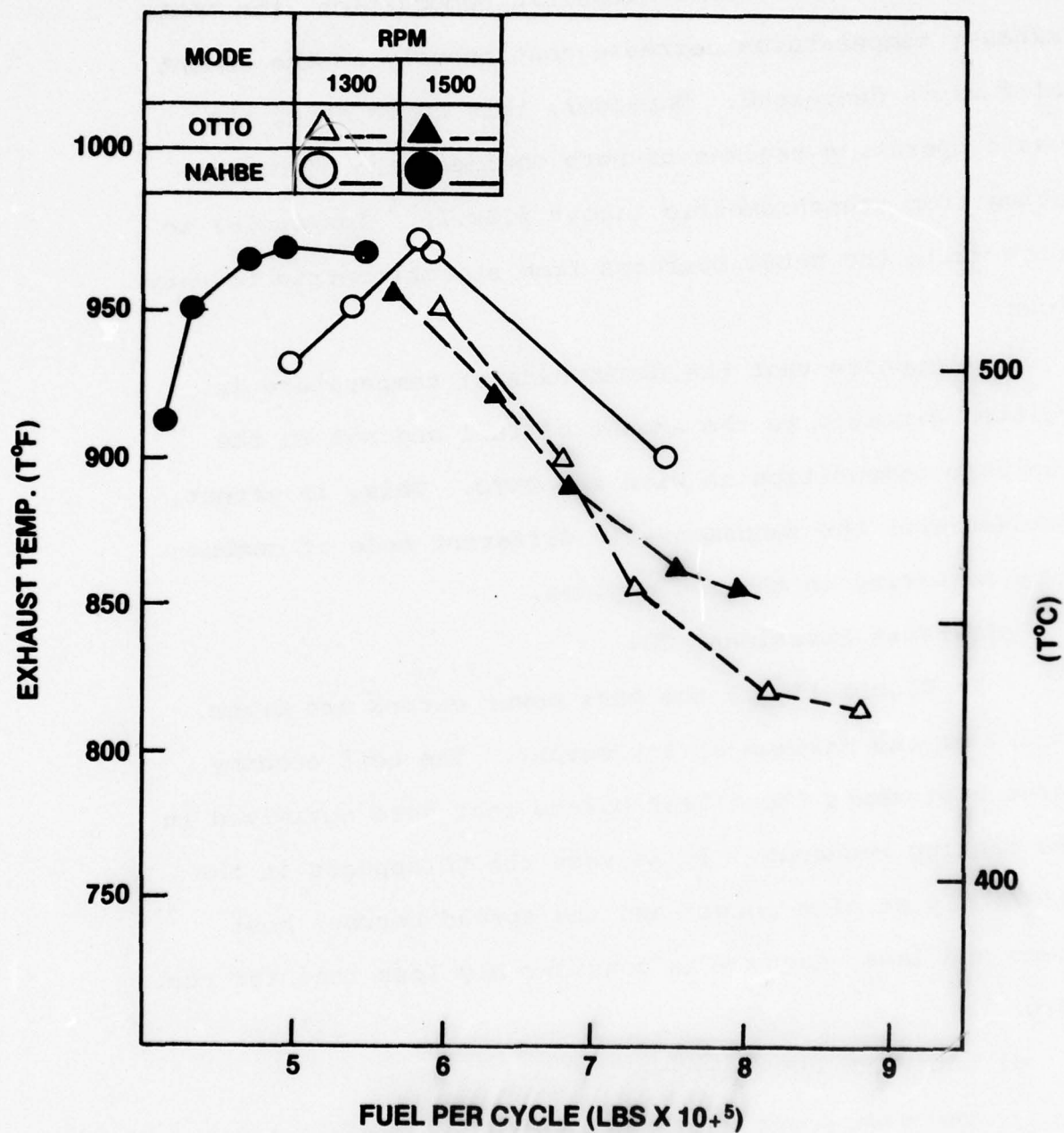


Fig. II-3.2
CFR comparison of exhaust gas temperatures

stoichiometric composition, exhaust temperatures continue to increase. Below stoichiometric composition, the NAHBE exhaust temperatures decrease continuously as the amount of fuel is decreased. Moreover, this curve shows the basic operating regimes of both engines, the OTTO operating from stoichiometric (about 5.8×10^{-5} lbs/cycle) to rich while the NAHBE operates from stoichiometric to very lean.

It appears that the NAHBE exhaust temperature is related directly to the amount of fuel and not to the fuel/air composition as with the OTTO. This, in effect, demonstrates the fundamentally different mode of combustion occurring in the two engines.

c) Exhaust Emissions, CO:

In Figure II-3.3 the best power curves are drawn at 2/3 of the maximum at any output. The best economy curve represents those test points that were optimized in the testing sequence. It is seen the CO appears in the NAHBE only at high output and the spread between best power and least economy is considerably less than for the OTTO.

d) Unburned Hydrocarbon:

The best power and best economy curves are drawn in Figure II-3.4 as in the previous figure. For the NAHBE there is no appreciable difference between best power and

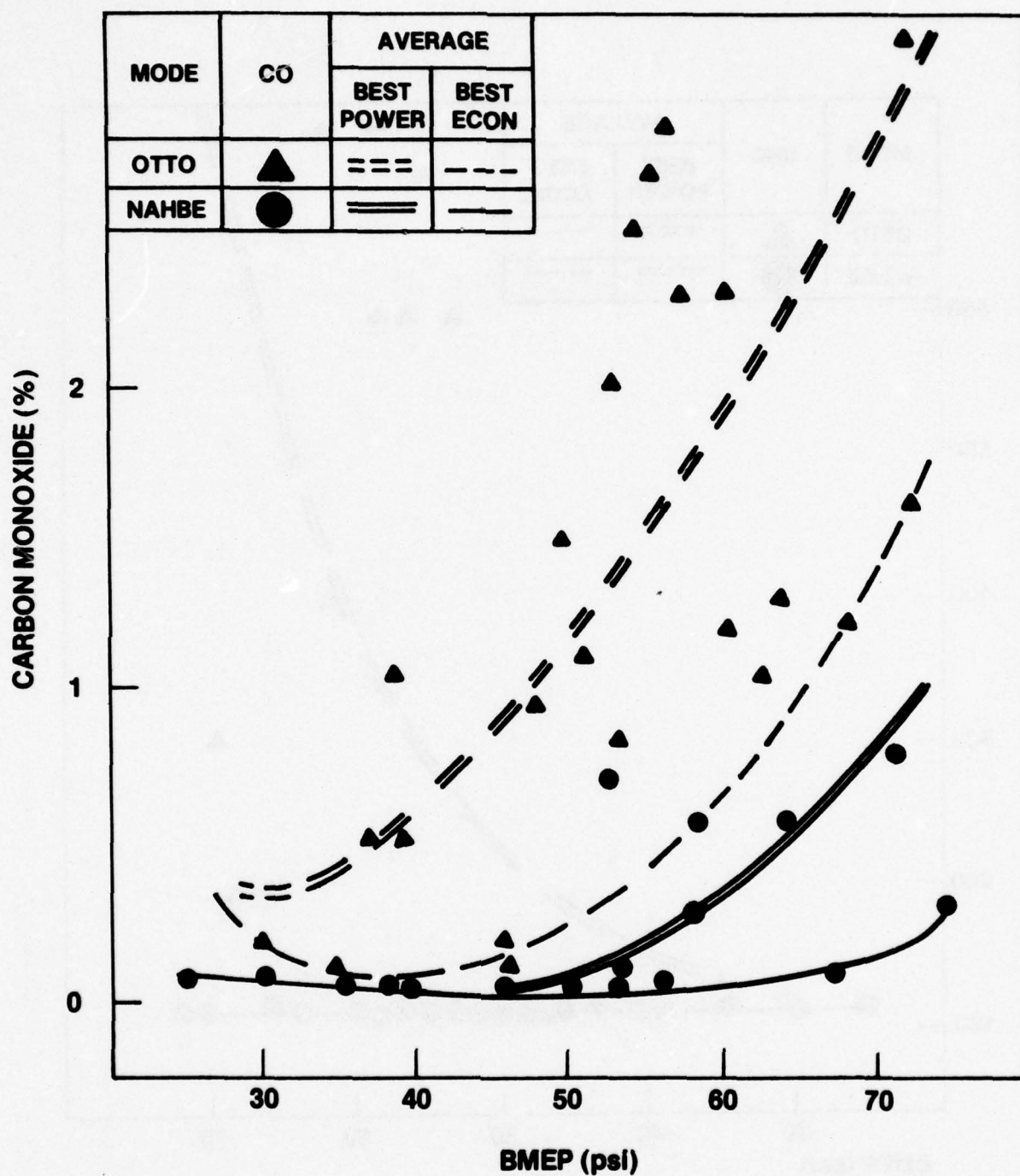


Fig. II-3.3
CFR comparison of carbon monoxide

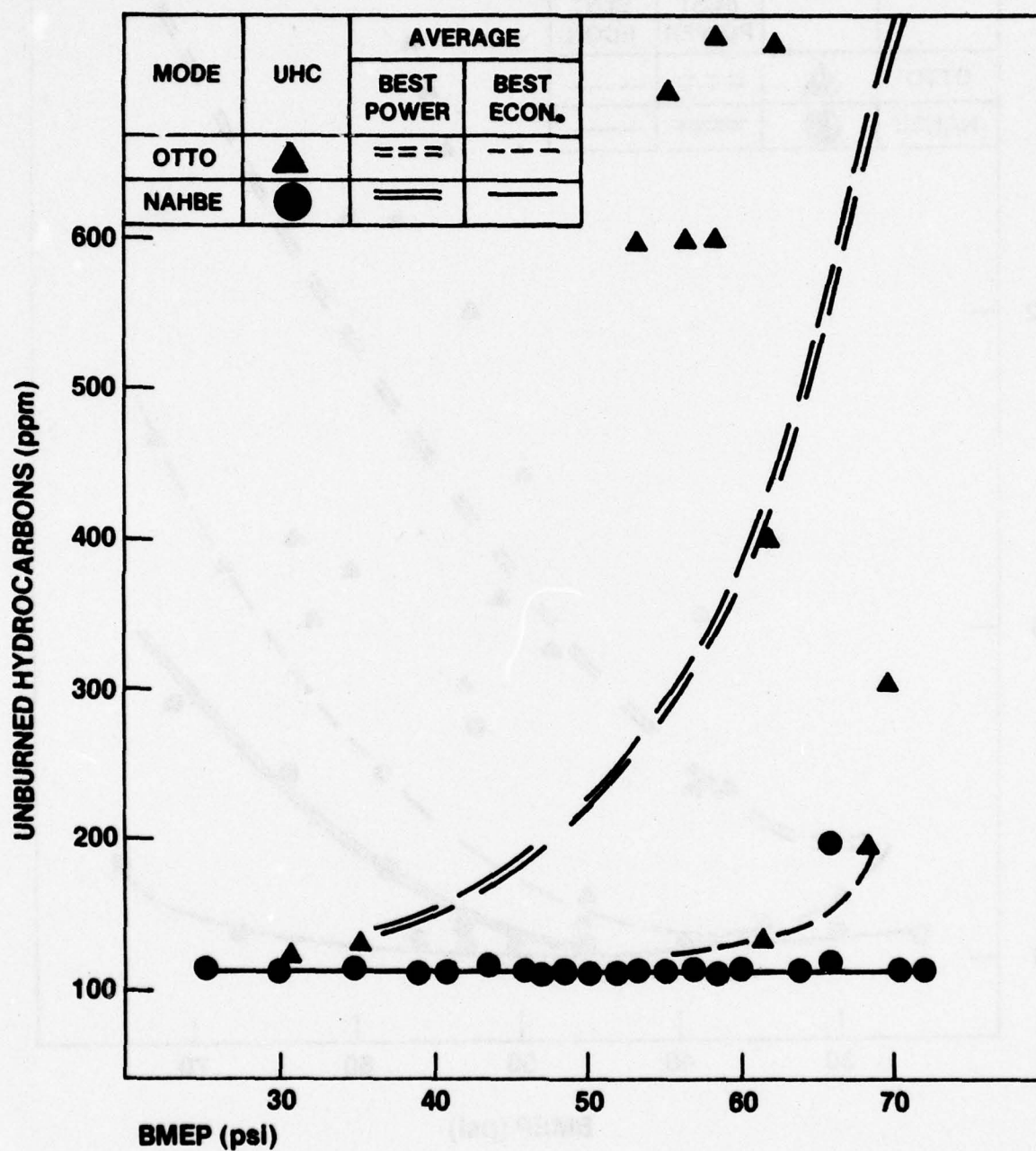


Fig. II-3.4
CFR comparison of unburned hydrocarbons

best economy. Only at low output and lean mixture does the OTTO begin to approach the completeness of combustion of the NAHBE that results in the low level of unburned hydrocarbon emitted in the exhaust.

e) Performance Characteristics:

Figure II-3.5, in which total horsepower and specific fuel consumption are compared at two different rpm, defines the distinct operating regimes for the OTTO and NAHBE modes. Again it is evident that the OTTO domain extends from rich mixture to slightly leaner than stoichiometric composition. Accepting similar volumetric efficiencies, the NAHBE domain begins near the end point of the OTTO and extends down to the limits of flamability for air-fuel mixtures.

It is seen that the NAHBE output is dependent on the quantity of fuel admitted and not on the air-fuel ratio of the OTTO. For example, at 1500 rpm for a total (or indicated) horsepower of 8 hp, the NAHBE consumes about 0.27 lbs of fuel per horsepower-hour while the OTTO shows a consumption of about 0.41. A later figure, Figure II-3.11, gives the results of all the tests of this series for all rpm.

In Figure II-3.6 the specific fuel consumption is given versus brake horsepower. For a given output the

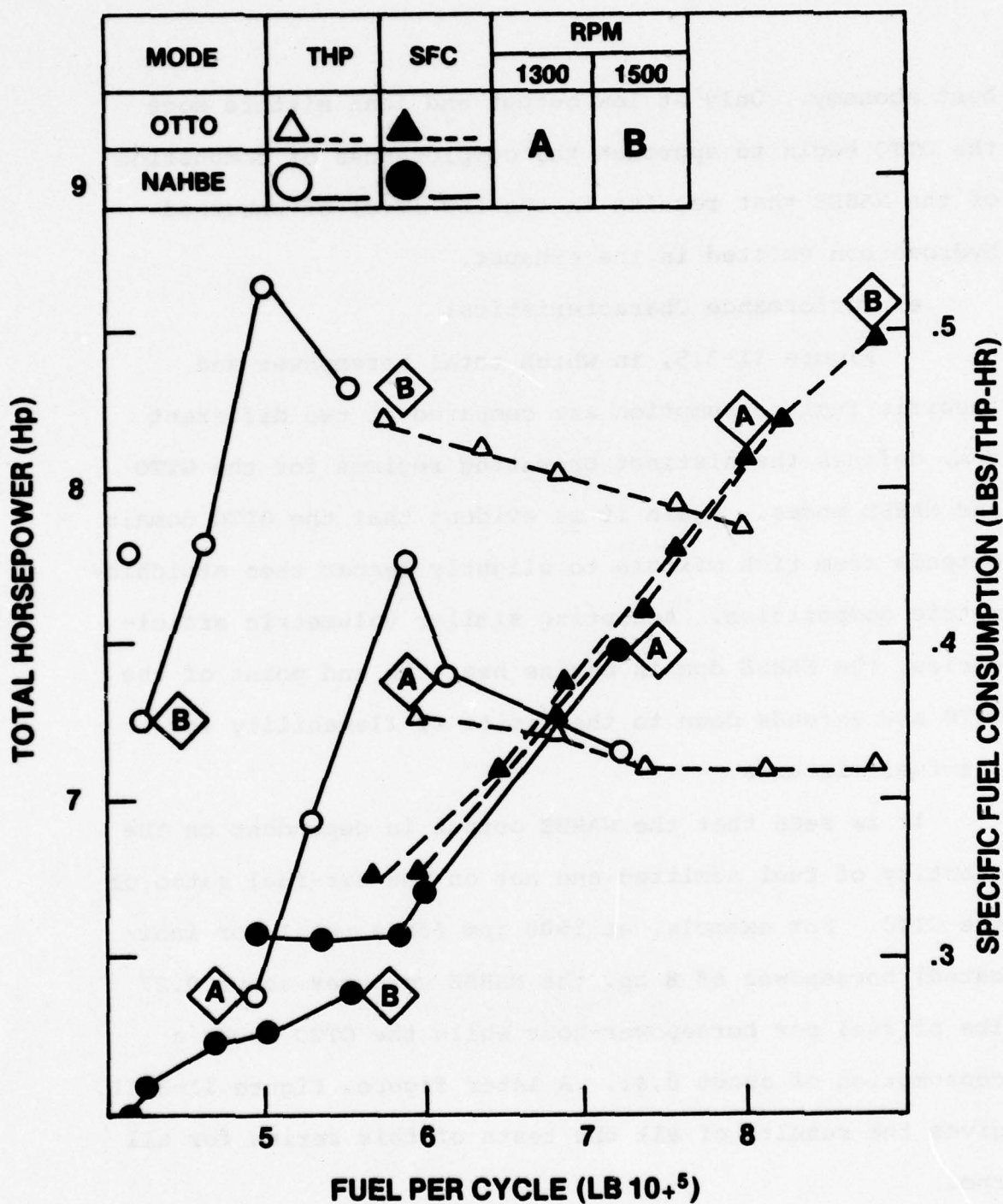


Fig. II-3.5
CFR comparison of total output horsepower
and specific fuel consumption

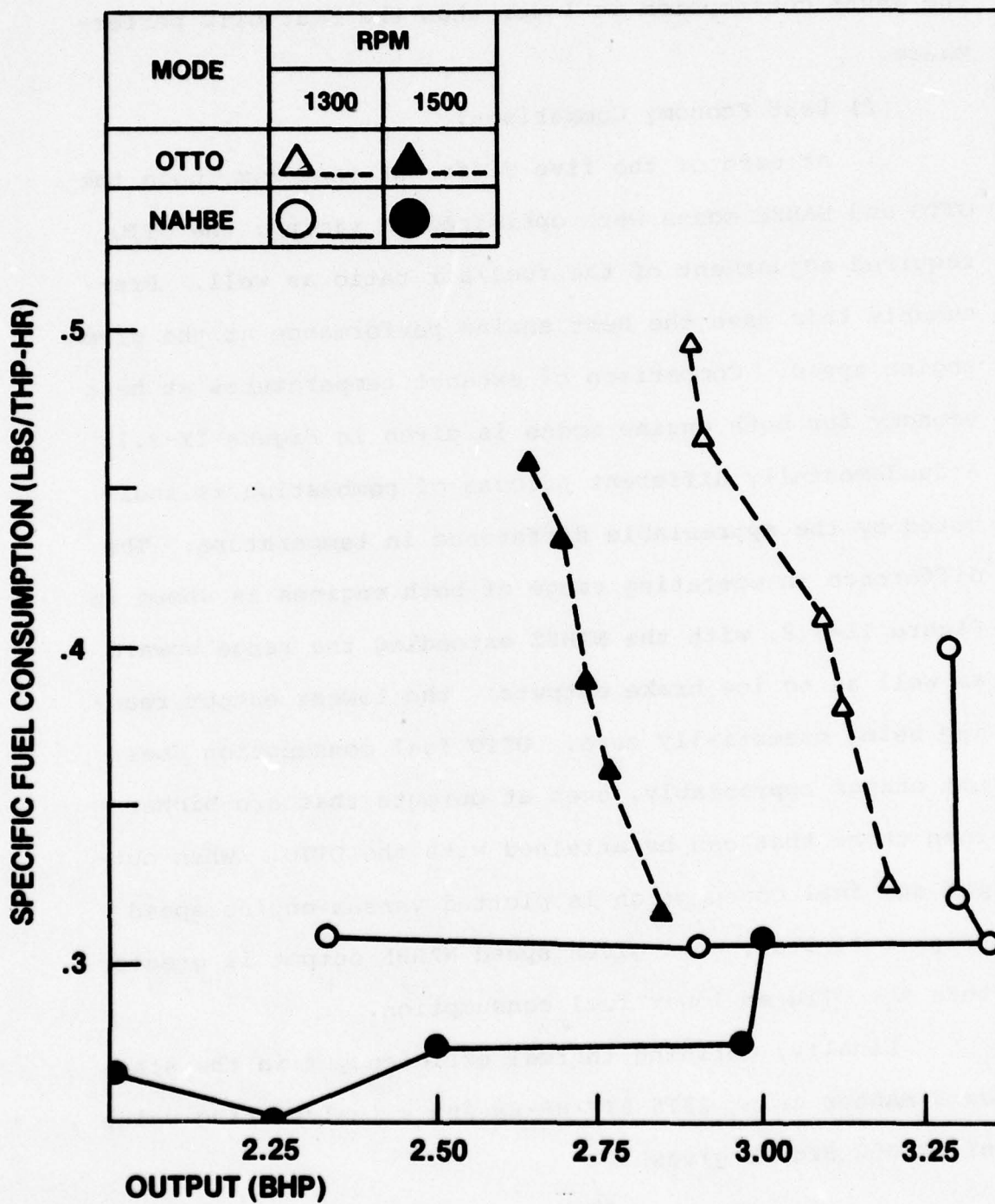


Fig. II-3.6
CFR comparison of specific fuel consumption

the NAHBE consumption is lower than the best OTTO performance.

f) Best Economy Comparison:

At each of the five different test rpm, both the OTTO and NAHBE modes were optimized in timing; the OTTO required adjustment of the fuel/air ratio as well. Presumably this gave the best engine performance at the given engine speed. Comparison of exhaust temperatures at best economy for both engine modes is given in Figure II-3.7. A fundamentally different process of combustion is indicated by the appreciable difference in temperature. The difference in operating range of both engines is shown in Figure II-3.8, with the NAHBE extending the range upward as well as to low brake outputs; the lowest output reading being essentially zero. OTTO fuel consumption does not change appreciably, even at outputs that are higher than those that can be attained with the OTTO. When output and fuel consumption is plotted versus engine speed (Figure II-3.9), at a given speed NAHBE output is greater than the OTTO at lower fuel consumption.

Finally, defining thermal efficiency η in the standard manner using 2575 BTU/HP-HR and a fuel heating value of 19,000 BTU/lb gives

$$\eta = \frac{2545}{19000 \times \text{SFC}} \times 100 \quad \text{II-3.1}$$

and percent improvement I of the NAHBE over the OTTO

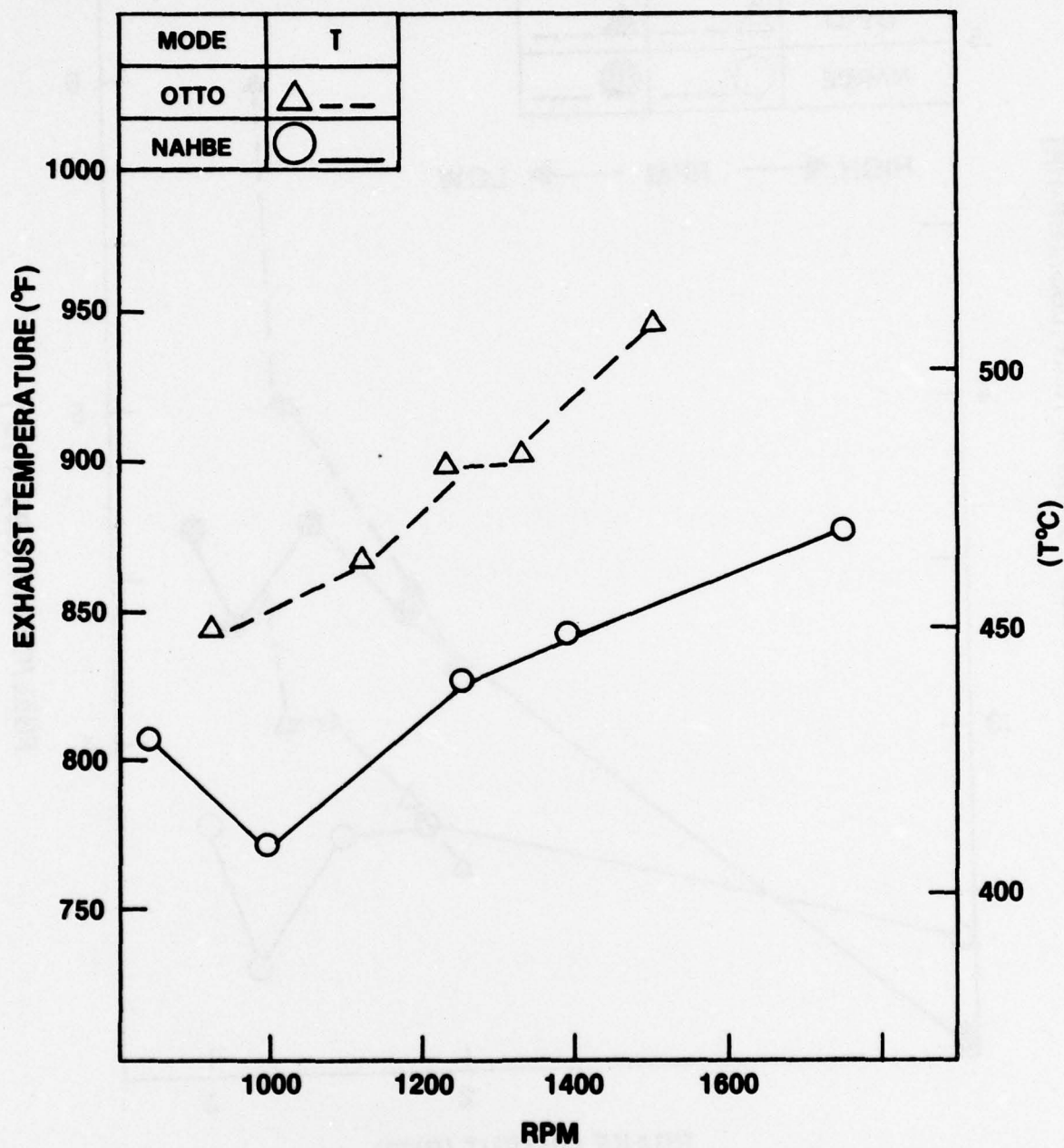


Fig. II-3.7
Best economy comparison of exhaust gas temperature

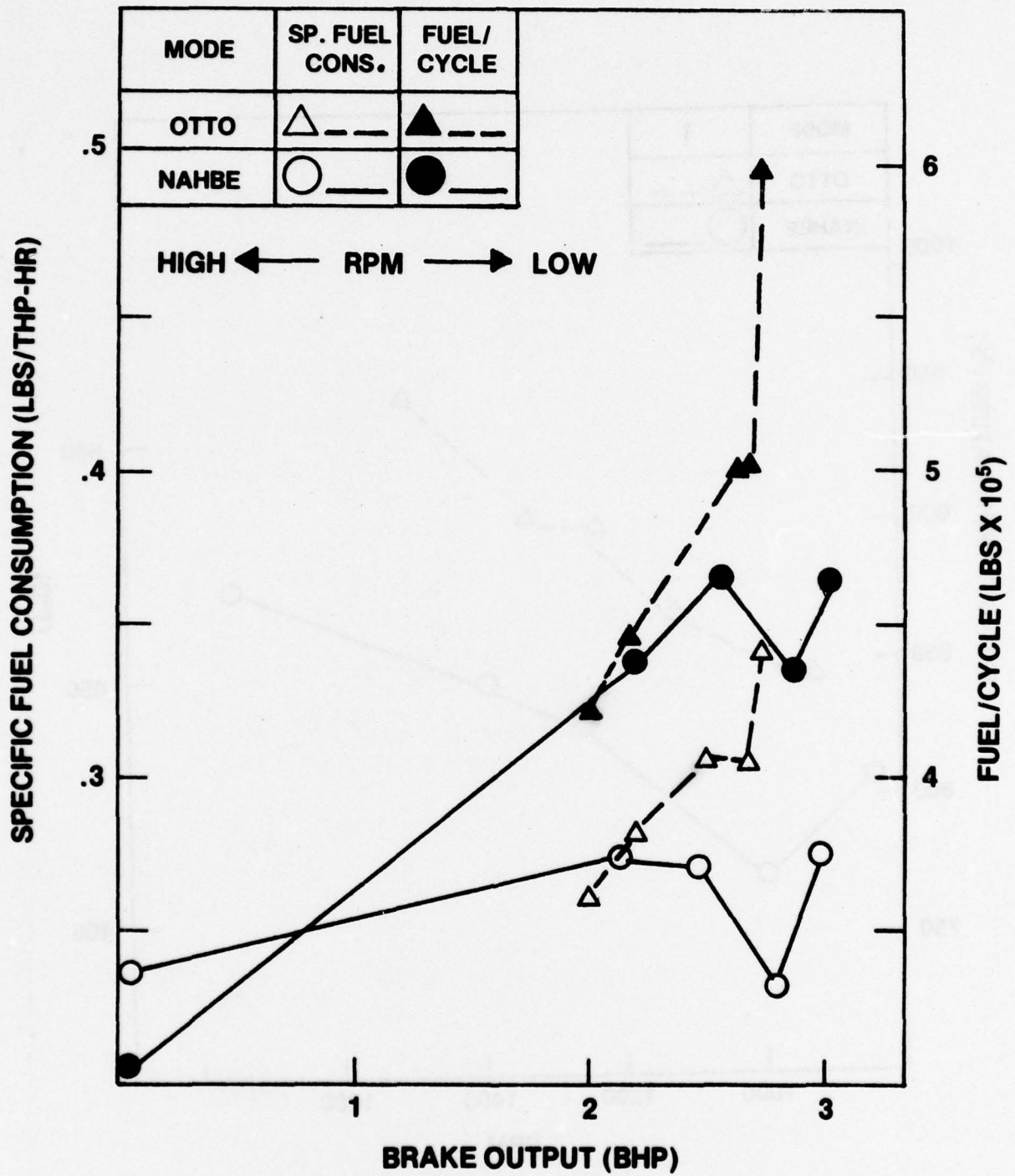


Fig. II-3.8

Best economy comparison of fuel consumption

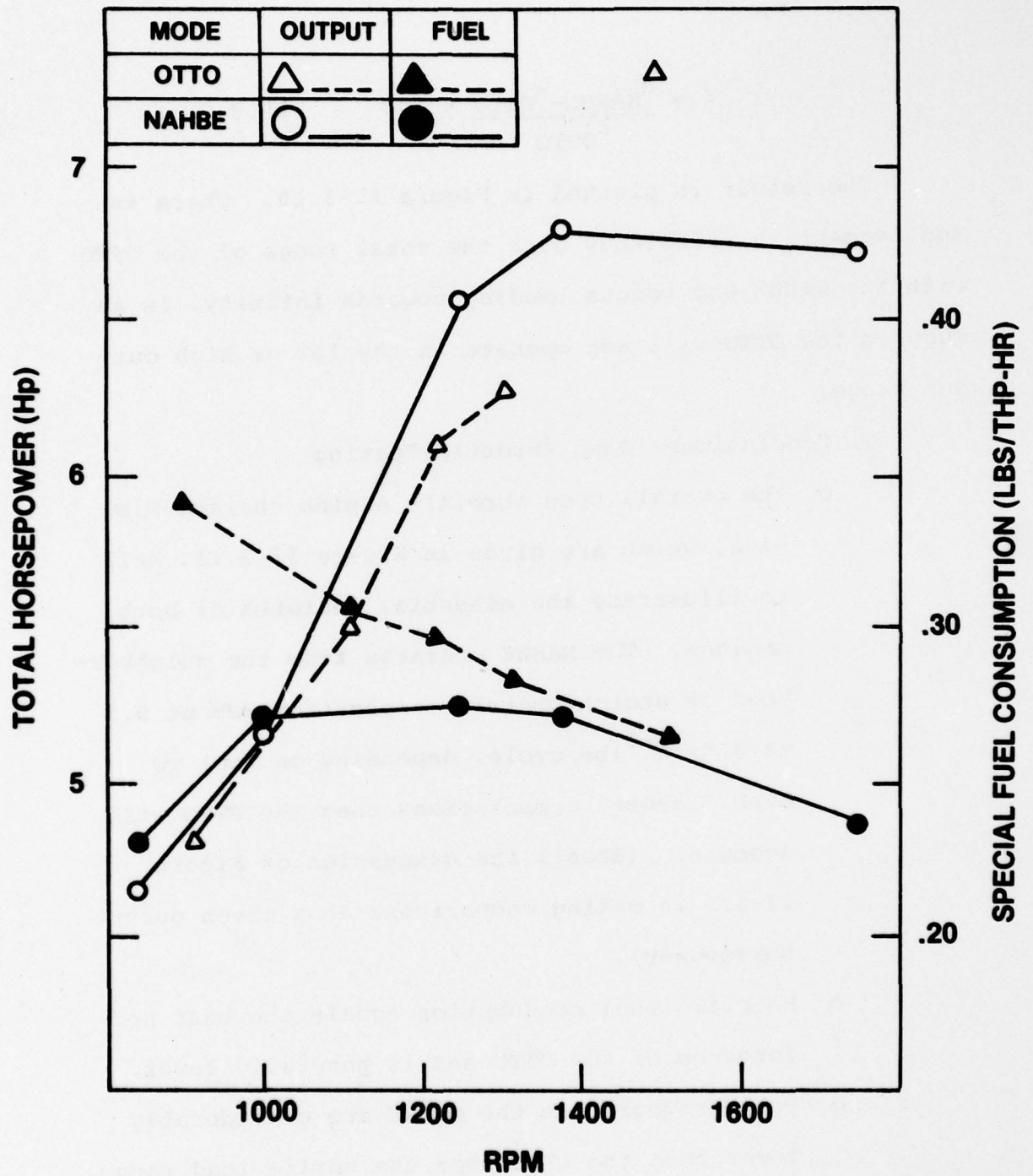


Fig. II-3.9
Best economy comparison of
total output and fuel consumption

$$I = \frac{\eta_{\text{NAHBE}} - \eta_{\text{OTTO}}}{\eta_{\text{OTTO}}} \times 100 \quad \text{II.3.2}$$

The result is plotted in Figure II-3.10. There is improvement in efficiency over the total range of the OTTO with the NAHBE end points tending towards infinity, in as much as the OTTO will not operate in the low or high output range.

g) Conclusions, Open Throttle Testing

- o The overall open throttle engine characteristics, which are given in Figure II-3.11, help to illustrate the essential features of both engines. The NAHBE operates from the neighborhood of stoichiometric composition (about 5.5 to 6.5×10^{-5} lbs/cycle, depending on rpm) to much "leaner" compositions than the OTTO will accept. (Recall the discussion of Figure II-3.5 in making comparisons at a given output horsepower).
- o Specific fuel consumption equals the best performance of the OTTO and is generally lower.
- o Peak pressures in the NAHBE are considerably lower than the OTTO over the entire load range.
- o NAHBE exhaust temperatures are proportional to the amount of fuel admitted while OTTO exhaust temperatures depend on the fuel/air mixture.

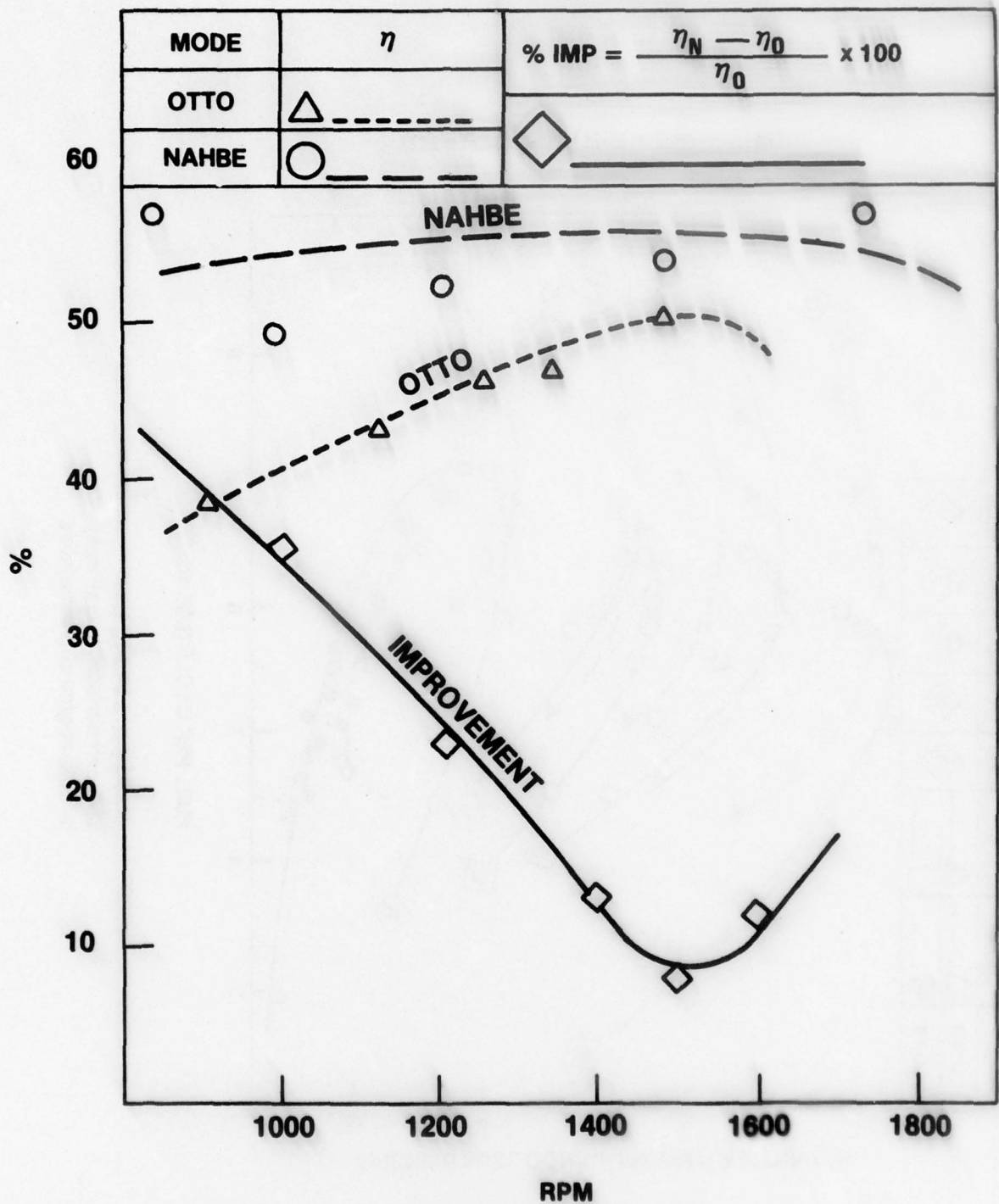


Fig. II-3.10
Best economy comparison of efficiency
and percent improvement

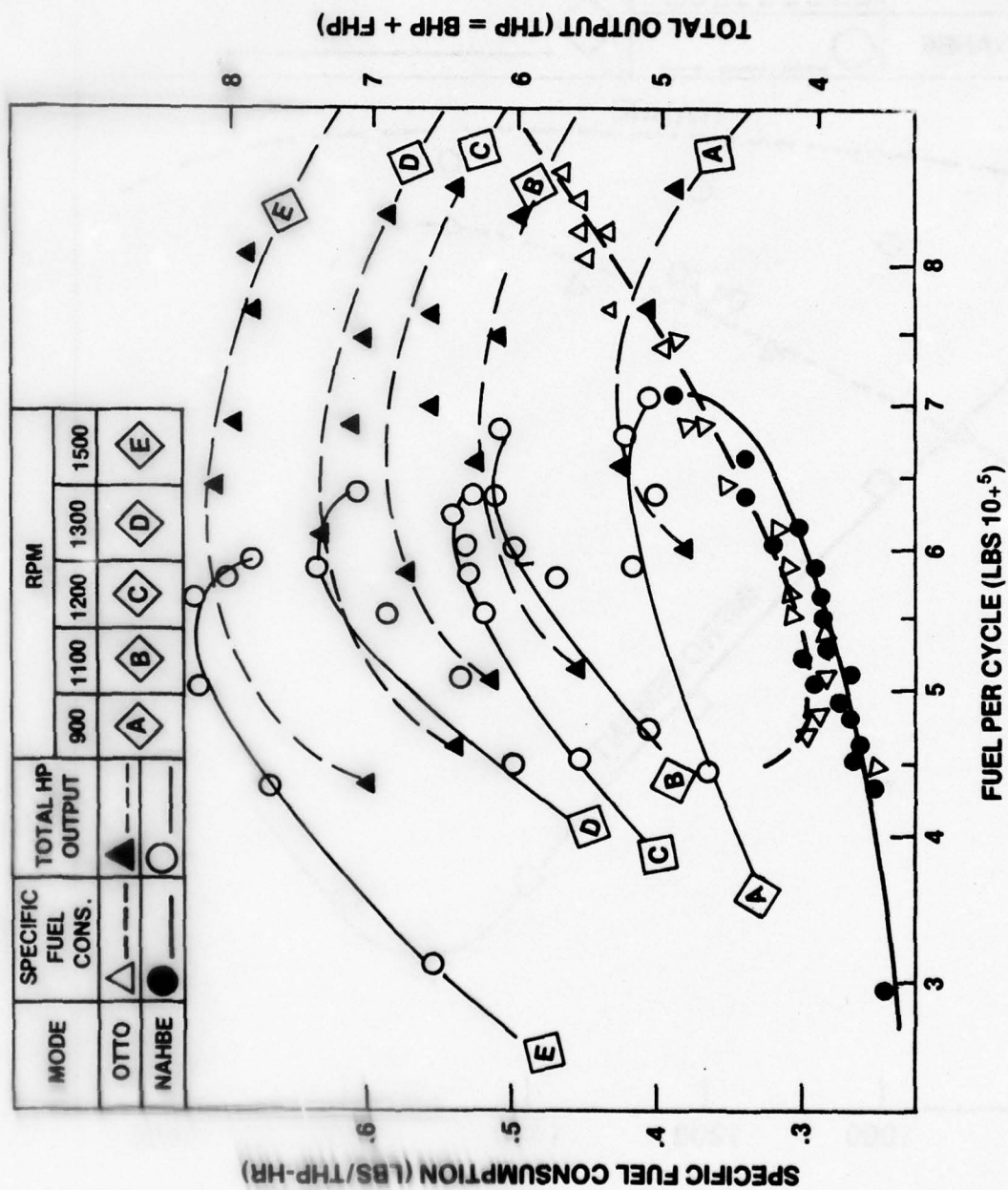


Fig. II-3.11
CFR comparison, overall open
throttle engine characteristics

- o Carbon monoxide and unburned hydrocarbon emissions in the NAHBE are lower than the OTTO over the entire range of output both at best power and best economy.
- o NAHBE thermal efficiency exceeds the OTTO over the entire range of the OTTO, moreover, the NAHBE will operate to both lower and higher brake loads than the OTTO.

4. Test Results, Throttled Engine Configuration

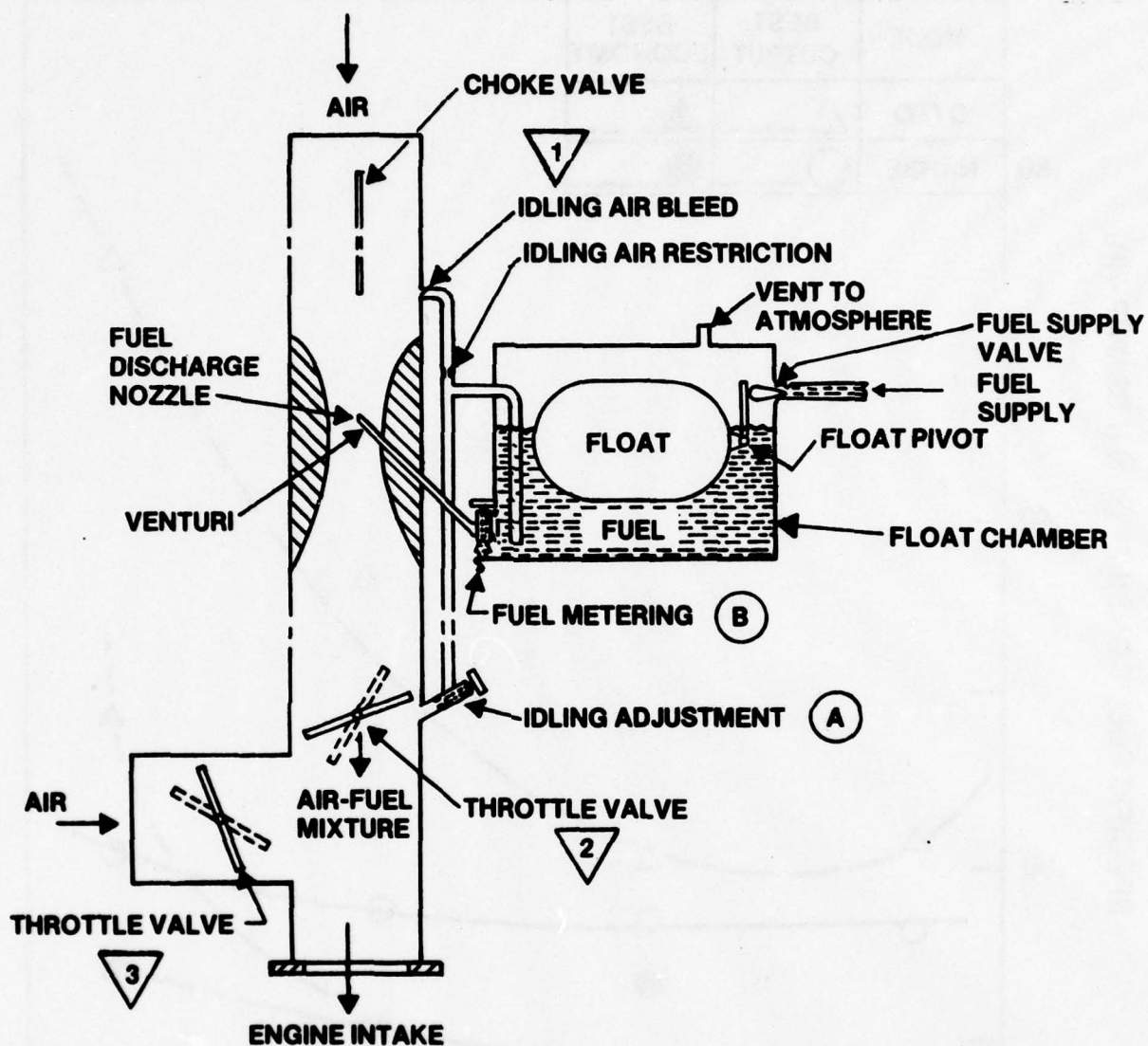
In order to compare both engines modes under other than full throttle conditions, a carburator with separate needle valves for control at idle and normal operation was fabricated and installed on the CFR engine (Figure 11-4.1). Both needle valves were used in the OTTO mode, while only the principle valve was used in the NAHBE mode.

Tests were run at four throttle settings: minimum output, 1/3, 2/3 and full throttle. Timing was optimized for NAHBE best output while both timing and fuel were optimized for best economy in the OTTO mode. In the NAHBE the air was throttled only in the bypass air supply (independent of the fuel supply); a fixed flow of air through the principle venturi-jet was used to supply fuel. See Figure II.4.1. Total control of metering in the NAHBE was through the principal metering needle valve. Operation in the OTTO configuration required that the bypass in Figure

II-4.1 be closed.

The results of Figures II-4.2 to 4.4 show that at best economy, the OTTO and NAHBE results are comparable at low loads and diverge rapidly above 2.3 horsepower. Figure II-4.2 shows that at best power output the NAHBE specific fuel consumption variation with throttle opening is slight: about 0.28 to 0.30 lbs/THP-HR. The OTTO variation, however, is from about 0.30 to about 0.50 lbs/THP-HR.

Figure II-4.4 shows the classic "best possible performance" for the OTTO. The NAHBE equals or exceeds the best possible OTTO over a wider range of operation.



OPERATION

OTTO — AIR FLOW: 1—OPEN, 2—THROTTLING, 3—CLOSED.
 FUEL FLOW: A—CALIBRATED BEST IDLING SETTING
 B—OPTIMIZED FOR EACH THROTTLE SETTING

NAHBE — AIR FLOW: 1—CLOSED WITH $\frac{1}{4}$ " DIA. BLEED HOLE
 2— $\frac{1}{2}$ OPEN
 3—THROTTLING
 FUEL FLOW: A—CLOSED
 B—VARIABLE OUTPUT METERING CONTROL

Fig. II-4.1
 NAHBE and OTTO throttling scheme

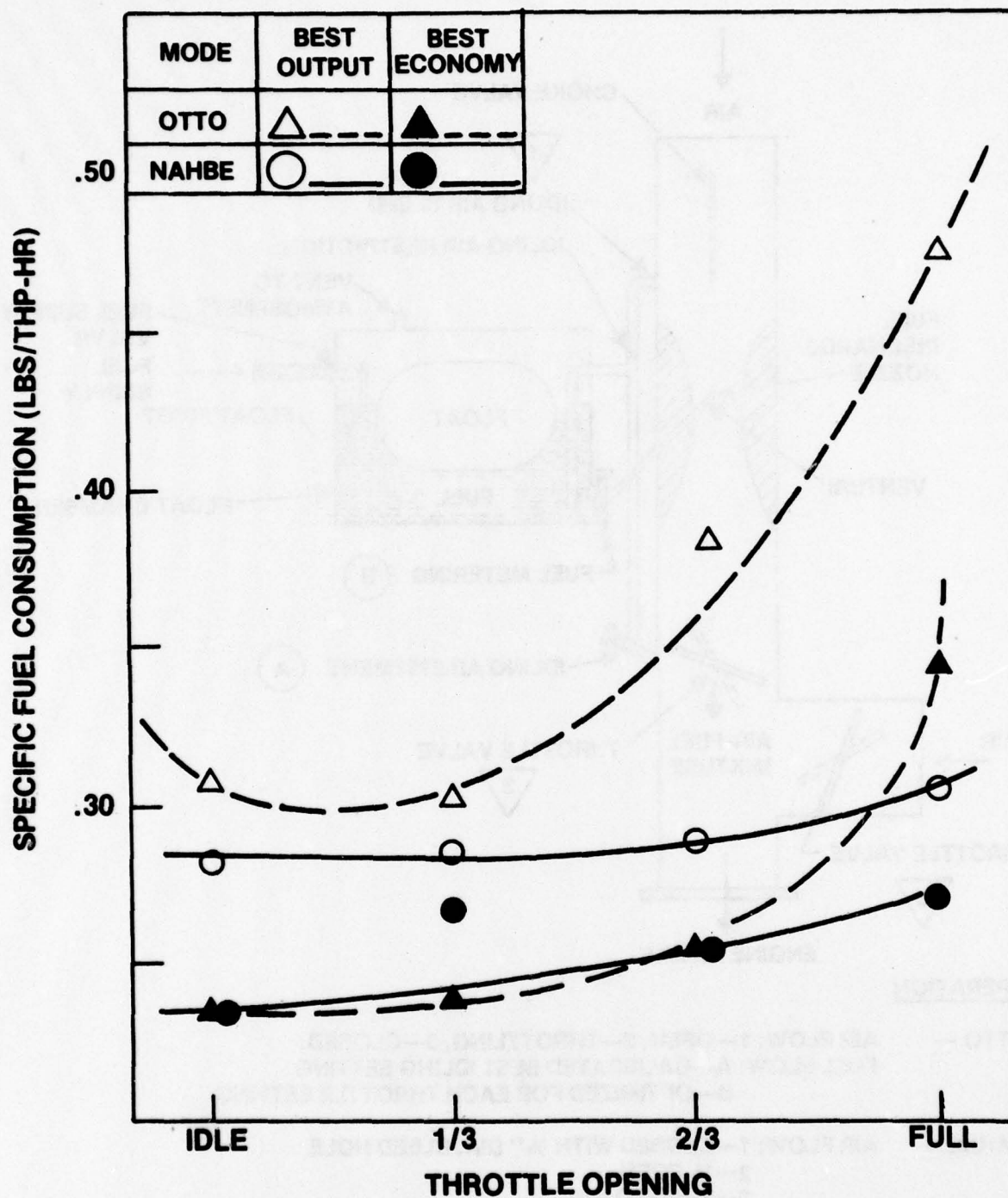


Fig. II-4.2
Throttled engine comparison of
specific fuel consumption

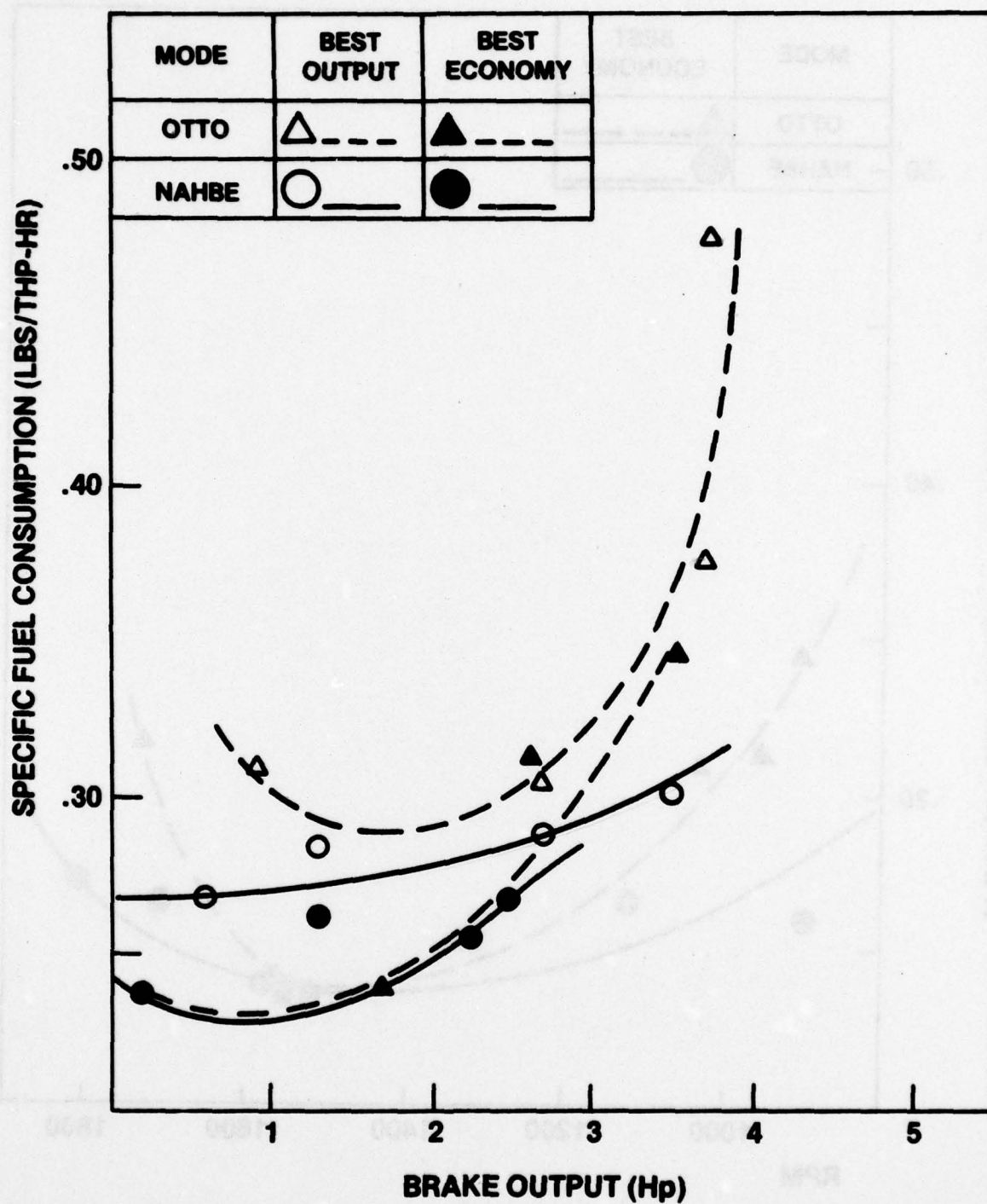


Fig. II-4.3

Throttled engine comparison of brake output

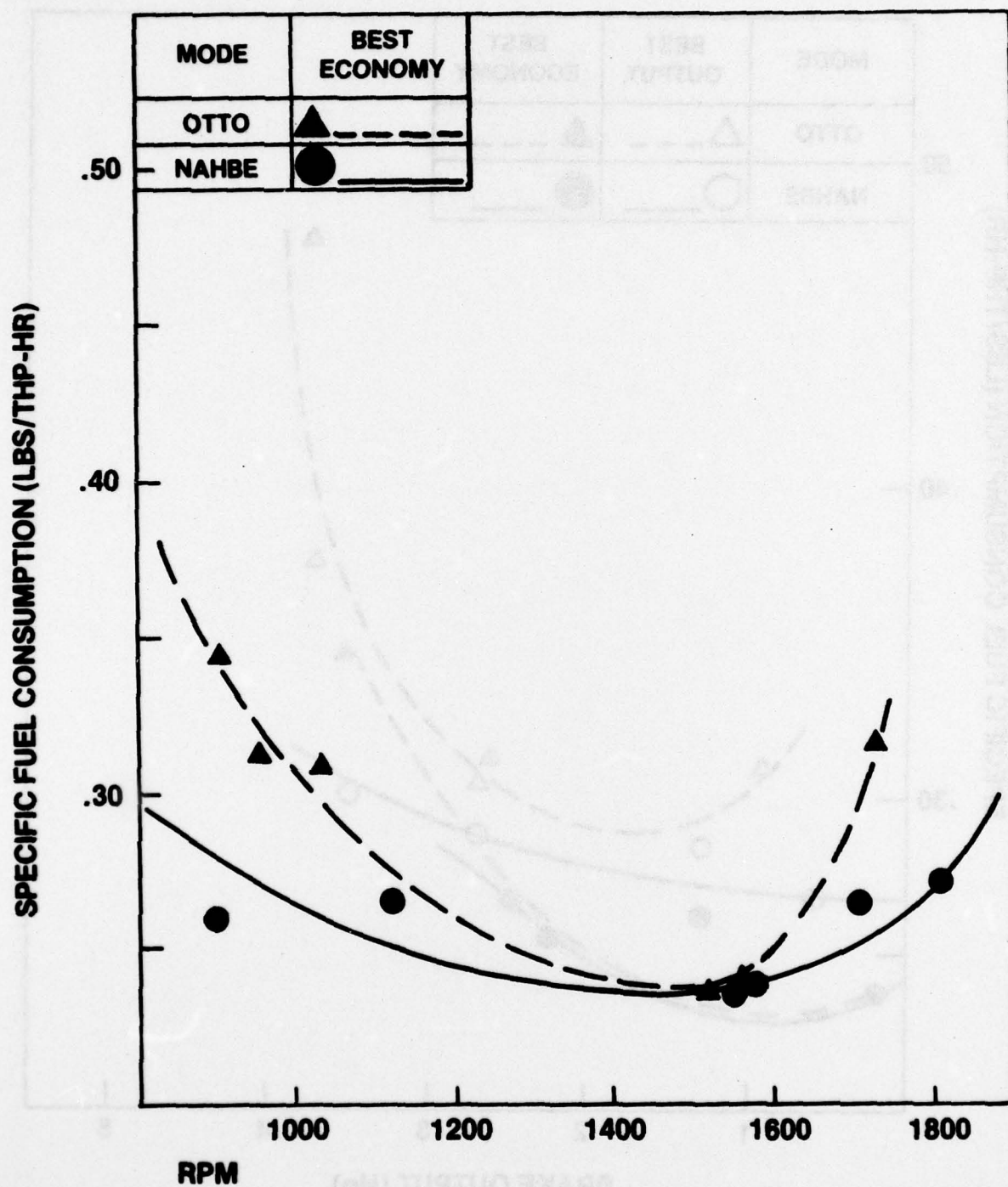


Fig. II-4.4
Throttled engine comparison of
specific fuel consumption

APPENDIX III

OPTICAL STUDY OF THE NAHBE MODE OF COMBUSTION

1. Tests Variables

This optical study was carried out using a high speed television camera to take the photographs desired. Engine operating conditions were varied to allow evaluation of the effect of each set of conditions on the combustion process. RPMs were adjusted over a range of 450-1600, fuel-to-air ratios varied from lean to rich, and loading conditions varied from low to high.

As was discussed previously, an overly rich fuel/air charge broke the chain of events characteristic of NAHBE combustion. As such, attention will be centered only on NAHBE combustion.

In analyzing the photographs of NAHBE combustion geometric orientation of the photographs is essential. Looking at the figures contained in this appendix, the fuel/air charge enters from the left and the spark plug is located off-center approximately one-third the cylinder width from the right cylinder wall.

In correlating the black-and-white photographs to the actual colors observed during testing white in the photographs corresponds to white and yellow combustion in the engine. Shades of grey in the combustion chamber correspond to the characteristic blue color of

complete combustion.

2. Optical Analysis, High Load

In observing the results of placing a high load on the engine with a dynamometer, Figures III-2.1 and 2.2 are representative photographs of the sequence under consideration. The engine was operated at approximately 600 rpm under a high load with a stoichiometric fuel/air charge being supplied.

Figure III-2.1 depicts combustion at reference time $t=0$. Combustion is intense and incomplete at this stage and most of the oxygen available in the combustion chamber has been used up by time $t=4$ msec, corresponding to the end of combustion in the OTTO cycle. Flow from the combustion chamber is entering the balancing chamber and the separation of flow at the corner of the pressure exchange cap is clearly visible.

Figure III-2.2 represents the progression of combustion at $t=10$ msec. The flow has been reflected by the balancing chamber geometry, bringing with it additional oxygen from the balancing chamber. A blue zone of combustion covering a total of approximately sixty percent of the combustion chamber surrounds a white-yellow zone centered around the spark plug location. Under this high load condition, combustion ended at this point.

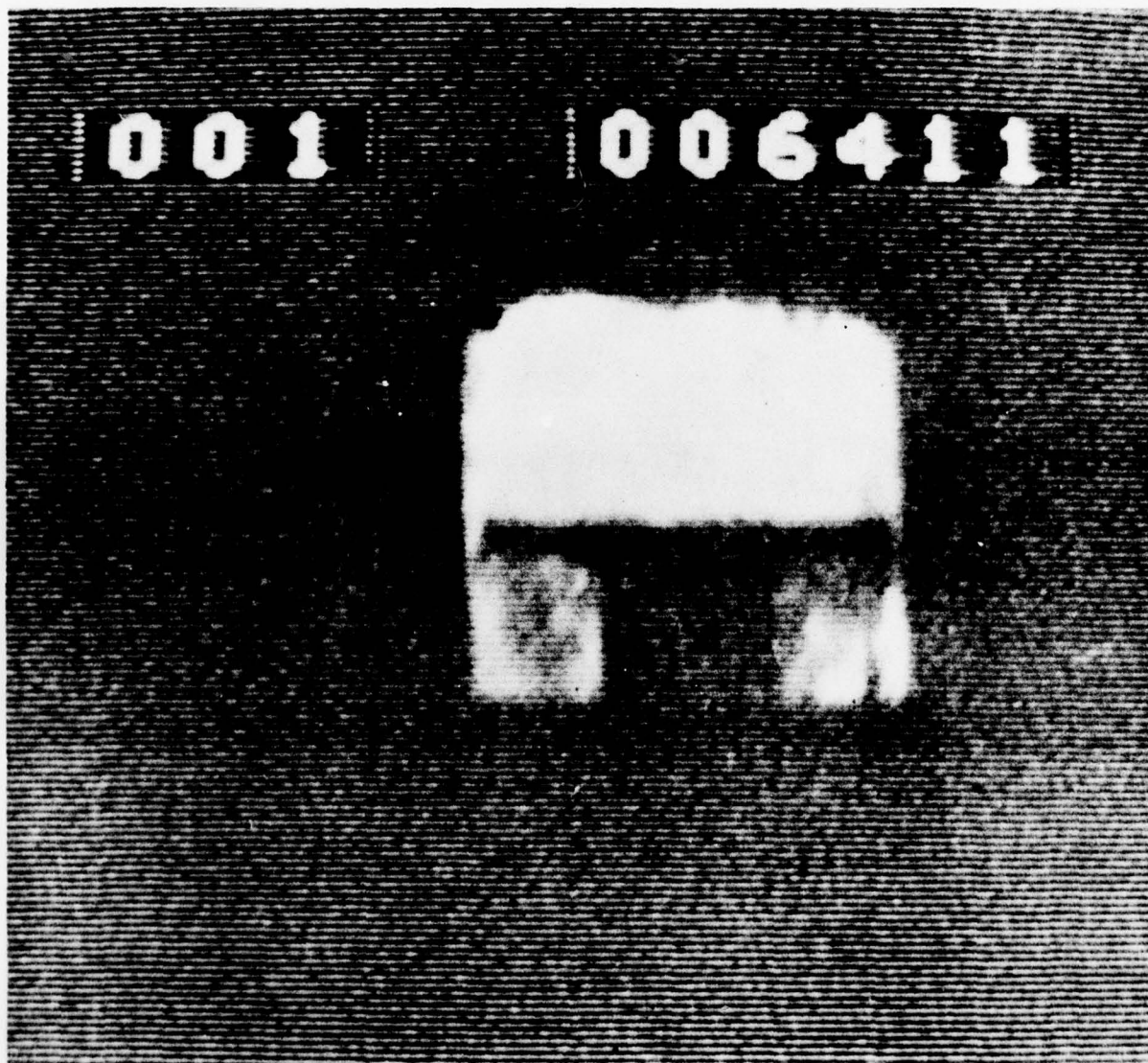


Fig. III-2.1

High Load Combustion, $t=0$

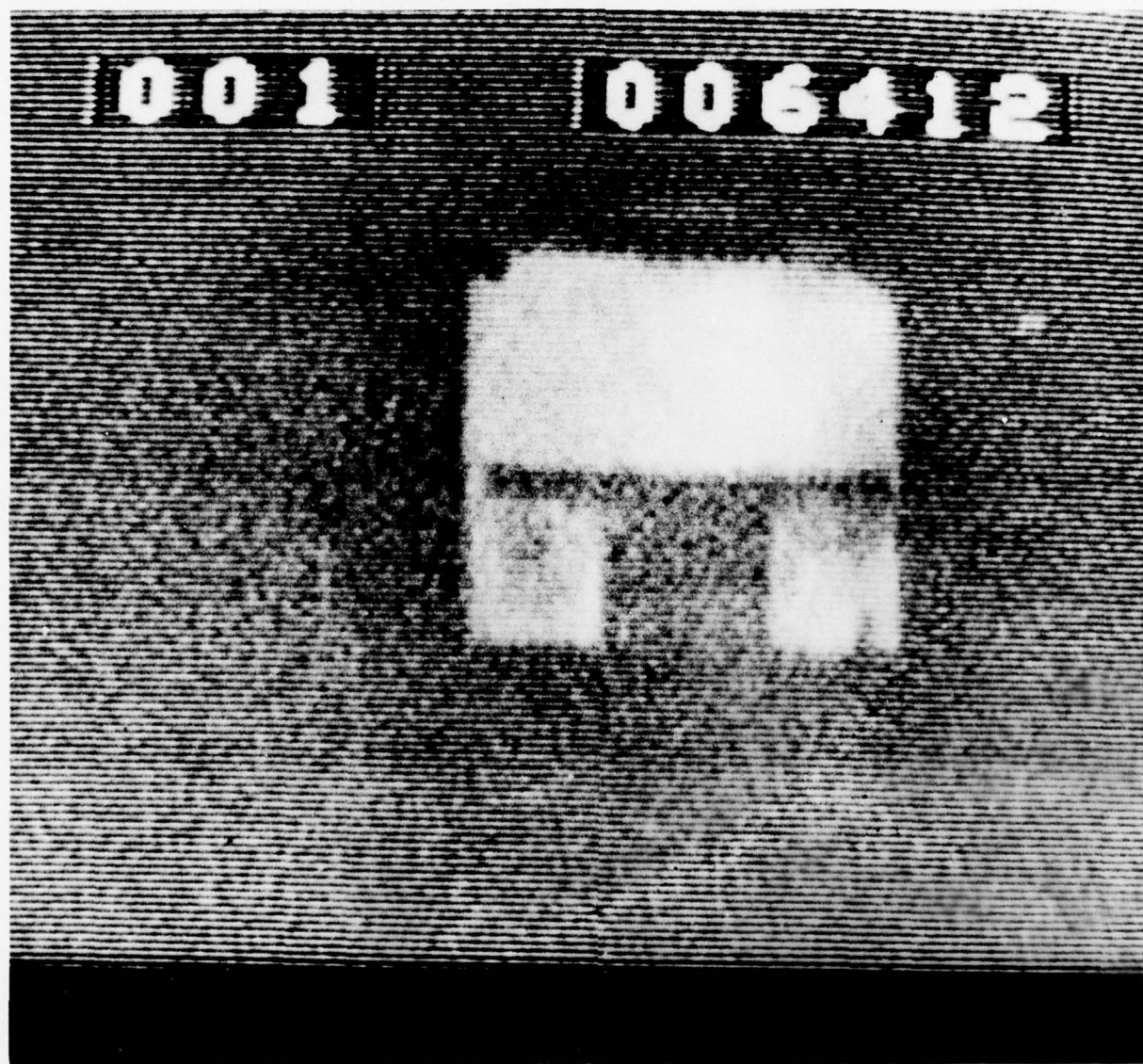


Fig. III-2.2

High Load Combustion, $t=10$ msec



Fig. III-3.1

Low Load Combustion, $t=0$

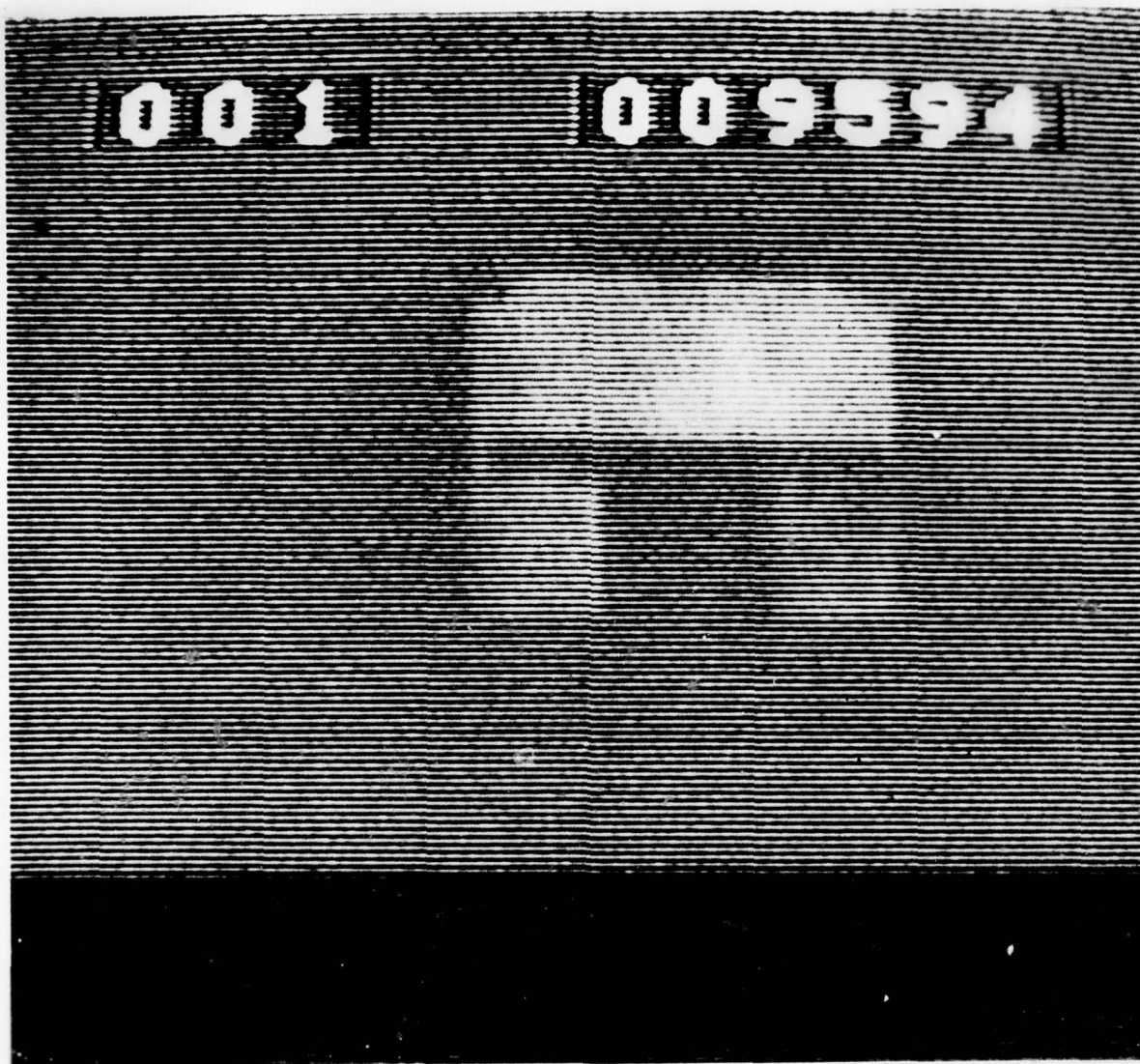


Fig. III-3.2

Low Load Combustion, $t=10$ msec



Fig. III-3.3

Low Load Condition, $t=20$ msec

3. Optical Analysis, Low Load

Representative results of placing the engine under a low load are shown in Figures III-3.1, 3.2, and 3.3. The engine was operated at approximately 1100 rpm using a fuel/air charge slightly leaner than stoichiometric composition.

Figure III-3.1 shows the combustion at reference time $t=0$. Combustion is less intense (hot) than under the high load condition. Shock compression waves from the combustion chamber have transited the gap between the pressure exchange cap and the cylinder wall and have entered the balancing chamber.

Figure III-3.2 illustrates combustion progression at $t=10$ msec. Nearly the same conditions exist here as at the end of NAHBE combustion under the high load condition just discussed. However, under low load conditions, combustion continues to completion at $t=20$ msec, shown in Figure III-3.3. The entire combustion zone is blue in color, characteristic of complete combustion.

4. Conclusions

The optical studies performed using high speed photography clearly show the presence of a large blue combustion zone in the NAHBE, in all cases larger than any such zone that arises in the OTTO only under low load conditions. This blue combustion zone is evidence

that additional oxygen is being supplied to the combustion chamber in the NAHBE.

When combustion begins a large pressure differential exists between the combustion and balancing chambers, preventing the oxygen in the balancing chamber from entering the combustion zone. However, the evidence of oxygen being supplied from the balancing chamber indicates that this pressure differential must have been reversed. Consequently, this proves that pressure exchange has occurred, lowering the pressure in the combustion chamber and raising the pressure in the balancing chamber to some level higher than in the combustion chamber. This process then allows oxygen to flow from the high pressure region in the balancing chamber to the low pressure region in the combustion chamber and thus carry combustion to a correspondingly more complete stage.

In summary, the mechanism of pressure exchange has been shown to exist. A more detailed study of the NAHBE combustion process would result in a more thorough understanding on which to base future optimization modifications.

UNCLASSIFIED

SECURITY CLASSIFICATION OF THIS PAGE (When Data Entered)

14 REPORT DOCUMENTATION PAGE		READ INSTRUCTIONS BEFORE COMPLETING FORM	
1. REPORT NUMBER U.S.N.A. - TSPR; no. 98 (1977)	2. GOVT ACCESSION NO.	3. RECIPIENT'S CATALOG NUMBER 9 Rept.	
4. TITLE (and Subtitle) PERFORMANCE ANALYSIS OF A MODIFIED INTERNAL COMBUSTION ENGINE.		5. TYPE OF REPORT & PERIOD COVERED Interim 1976-1977.	
		6. PERFORMING ORG. REPORT NUMBER	
7. AUTHOR(s) Timothy Lee/Whited,		8. CONTRACT OR GRANT NUMBER(s)	
9. PERFORMING ORGANIZATION NAME AND ADDRESS United States. Naval Academy Annapolis, Md. 21402		10. PROGRAM ELEMENT, PROJECT, TASK AREA & WORK UNIT NUMBERS	
11. CONTROLLING OFFICE NAME AND ADDRESS United States. Naval Academy Annapolis, Md. 21402.		12. REPORT DATE 23 May 1977	
		13. NUMBER OF PAGES 85	
14. MONITORING AGENCY NAME & ADDRESS (if different from Controlling Office) 12 88 p.		15. SECURITY CLASS. (of this report) UNCLASSIFIED.	
		15a. DECLASSIFICATION/DOWNGRADING SCHEDULE	
16. DISTRIBUTION STATEMENT (of this Report) This document has been approved for public release; its distribution is UNLIMITED.			
17. DISTRIBUTION STATEMENT (of the abstract entered in Block 20, if different from Report) This document has been approved for public release; its distribution is UNLIMITED.			
18. SUPPLEMENTARY NOTES Presented to the Chairman of the Trident Scholars of the U.S. Naval Academy.			
19. KEY WORDS (Continue on reverse side if necessary and identify by block number) Combustion research. Combustion engines.			
20. ABSTRACT (Continue on reverse side if necessary and identify by block number) The preliminary experimental investigations have already demonstrated that the new, controlled heat balanced cycles of the internal combustion engine can avoid exhausting pollutants to the environment by utilizing a clean, time dependent process of combustion, with pressure exchange. It is the overall objective of this study to show that pressure exchange is indeed the process responsible for the time dependent combustion that occurs in the Naval Academy Heat Balanced Engine (NAHBE).			

OVER !!

DD FORM 1 JAN 73 1473

EDITION OF 1 NOV 65 IS OBSOLETE

S/N 0102-LF-014-6601

UNCLASSIFIED.

SECURITY CLASSIFICATION OF THIS PAGE (When Data Entered)

245-600

JB

UNCLASSIFIED.

SECURITY CLASSIFICATION OF THIS PAGE (When Data Entered)

This report gives the state of the art of the Naval Academy Heat Balanced engine in terms of its theoretical basis, laboratory tests of a Combustion Fuel Research (CFR) engine; preliminary demonstration of a multi-cylinder engine - and optical testing of a single-cylinder, transparent engine. The paper details technical descriptions, drawings, etc.

In the future experiments, more sophisticated optical methods, Color Schlieren and holographic interferometry will be employed. Techniques such as these will permit detailed wave analysis and result in a more thorough understanding of the combustion process in the NAHBE cycle.

o - o